CONF-9510292--2

REVIEW OF COMPUTATIONAL THERMAL-HYDRAULIC MODELING

By

R. H. Keefer and L. W. Keeton

Presented at

EPRI Meeting on
Improving the Understanding and Control of
Corrosion on the Secondary-Side of Steam Generators

Held at
Airlie House, Airlie, Virginia
October 9-13, 1995

Bettis Power Laboratory
West Mifflin, PA 15122-0079

Operated for the U. S. Department of Energy
by WESTINGHOUSE ELECTRIC CORPORATION

DISCLAIMER

Review of Computational Thermal-Hydraulic Modeling

R. H. Keefer[1] and D. W. Keeton[1]

ABSTRACT

Corrosion of heat transfer tubing in nuclear steam generators has been a persistent problem in the power generation industry, assuming many different forms over the years depending on chemistry and operating conditions. Whatever the corrosion mechanism, a fundamental understanding of the process is essential to establish effective management strategies. To gain this fundamental understanding requires an integrated investigative approach that merges technology from many diverse scientific disciplines.

An important aspect of an integrated approach is characterization of the corrosive environment at high temperature. This begins with a thorough understanding of local thermal-hydraulic conditions, since they affect deposit formation, chemical concentration, and ultimately corrosion. Computational Fluid Dynamics (CFD) can and should play an important role in characterizing the thermal-hydraulic environment and in predicting the consequences of that environment. The evolution of CFD technology now allows accurate calculation of steam generator thermal-hydraulic conditions and the resulting sludge deposit profiles. Similar calculations are also possible for model boilers, so that tests can be designed to be prototypic of the heat exchanger environment they are supposed to simulate. This paper illustrates the utility of CFD technology by way of examples in each of these two areas. This technology can be further extended to produce more detailed local calculations of the chemical environment in support plate crevices, beneath thick deposits on tubes, and deep in tubesheet sludge piles. Knowledge of this local chemical environment will provide the foundation for development of mechanistic corrosion models, which can be used to optimize inspection and cleaning schedules and focus the search for a viable fix.

KEY WORDS: thermal-hydraulics, computational fluid dynamics, steam generator, corrosion

INTRODUCTION

Development of effective corrosion management strategies requires a detailed understanding of the corrosion sensitivities over the range of conditions likely to be encountered in a steam generator. Much of this knowledge must be obtained from laboratory corrosion tests, which then need to be extrapolated to evaluate performance of the heat exchanger tubing. To accomplish this extrapolation, the local chemical and electrochemical environment in both the test and the heat exchanger must be well characterized.

Environmental definition begins with a thorough understanding of the local thermal-hydraulic conditions, since they affect deposit formation, chemical concentration, and ultimately corrosion. Computational fluid dynamics

---

[1]Bettis Power Laboratory, West Mifflin, Pennsylvania, USA

DISCLAIMER

Portions of this document may be illegible in electronic image products. Images are produced from the best available original document.

will play an important role in characterizing the thermal-hydraulic environment and can aid in predicting the consequences, such as localized corrosive conditions, that can result from that environment.

The term Computational Fluid Dynamics (CFD) has become a catchall phrase used to describe a general methodology for attacking complex problems in fluid mechanics and heat transfer. In this 'computational' or 'numerical' approach to problem solving, the (usually partial) differential equations and associated boundary conditions that govern a process of interest are solved numerically (as opposed to theoretically), in a specially written computer program or code.

EPRI's ATHOS3 program is a CFD tool that is widely used in the nuclear power industry to perform three-dimensional, steady-state and transient, thermal-hydraulic analyses of PWR steam generators.[1] It is applicable to all the most commonly found recirculating-type U-tube (UTSG) and once-through (OTSG) steam generators and it has been extensively validated. ATHOS3 allows accurate calculation of steam generator thermal-hydraulic conditions and, with additional post-processing, resulting sludge deposit profiles. With some modification, similar calculations are also possible for model boilers. Development of this analysis capability would help eliminate some of the uncertainty as to whether tests and devices are adequate simulations of the phenomena of interest, a question that has often plagued past laboratory experiments. This is an important next step that should be taken to help researchers design tests prototypic of the heat exchanger environment they are supposed to simulate, facilitate interpretation of the results, and aid development of remedial fixes such as an inhibitor.

Discussed below are two case studies to illustrate the utility of this technology: (1) an ATHOS3 calculation of steam generator performance and comparison of calculated deposit profiles to measured deposit patterns and (2) a calculation of thermal-hydraulic performance for a generic model boiler with a simple enhanced concentration device.

CFD CALCULATION OF STEAM GENERATOR PERFORMANCE

Background

Keeton, et al. have demonstrated a model that can be integrated into ATHOS3 to estimate the relative amounts of sludge expected to accumulate in various regions of a steam generator.[2] With this technology, sludge deposit profiles can be calculated at every node used to model the steam generator and examined with thermal-hydraulic parameters to identify regions where excessive deposit formation could introduce a corrosion concern.

Review of Sludge Model

In the model, deposition and reentrainment rates are evaluated for single, assumed steady state values of particulate concentration and deposit thickness. The output from the model is the calculated ratio of deposition rate to reentrainment rate. When multiplied by the sludge concentration (mass fraction) in the boiler water, this deposition to reentrainment ratio represents the steady state mass (per unit surface area) of the deposit.[3]

The deposition and reentrainment coefficients depend upon the physical processes considered. The physical processes accounted for in these physical models are:

1. boiling enhanced deposition
2. turbulent deposition
3. gravitational settling
4. shear induced reentrainment of deposited particles

Detailed discussions of these mechanisms are not presented here but have been published previously.[2,3]

Case Considered

The model has previously been applied to consider a sample problem from the ATHOS3 documentation.[1] This sample problem corresponds closely to steam generators currently in use, designed by Combustion Engineering (CE). To further test and demonstrate the model, the analysis has been extended to consider two specific, commonly used PWR U-tube steam generator (UTSG) designs, viz: a Combustion Engineering (CE) System 80 (Figure 1) and a CE Series 67 (Figure 2), with both operating at their nominal/design 100% power conditions. These two UTSGs each have individual design features that make them unique relative to each other. As such, this makes them a fairly 'representative' and diverse pair upon which to demonstrate the model's **relative** abilities. In addition, they each have their geometry and operating conditions readily (and publicly) available in the ATHOS3 and (predecessor) ATHOS programs' documentation sets[1,4].

Results Obtained

The calculated thermal-hydraulic flow field and sludge deposition patterns, using the grid depicted in Figure 3, are presented in the form of various vector and contour plots in Figures 4 through 11.

For comparison purposes, Figures 12 through 15 show information pertaining to a recent tube rupture that occurred in a CE System 80 UTSG located at the Palo Verde Nuclear Generating Station, operated by the Arizona Public Service Company.[5] The utility has concluded that the tube rupture was caused by corrosion occurring beneath unanticipated and large (= thick) sludge deposits that formed on open tube surfaces in the steam generator's U-bend region. As a partial and first test of the sludge model, recent publicly-presented sludge deposit distribution data obtained after inspecting the CE System 80 unit (and other similar ones) are compared to the model's predictions.

Figures 12 and 13 show the vertical, radial and circumferential positions in the unit of the failed tube (row 117, column 144) and the location of the center of the approximately 8" long crack.

Figures 14 and 15 show the locations within two of the (six) CE System 80 units at the Palo Verde site (with the tube rupture having occurred in the 'SG22' unit depicted in Figure 15) where eddy-current inspection detected deposits on tubes of greater than a threshold amount of ~2 to 5 mils.

In Figures 12 through 15, it should be noted that:

- Vertically, the 8" crack in the ruptured Palo Verde CE System 80 tube is located at a position approximately mid-way between the two partial tube support plates, just below the inner edge of the top-most one (09H - Figure 12).

- Circumferentially, the ruptured tube is located at about the 40° mark from the tube symmetry plane, on the inlet side (Box 'B' in Figure 13).

- Radially, the ruptured tube is located at about 85% of the way between the centerline and the shroud, right at the partial support plate's inner edge (Figures 12 and 13).

Figures 4, 5 and 6 depict calculated inlet and outlet side sludge thickness patterns and mixture velocities (colored by vapor fraction), for the CE System 80 Integral Economizer design, at the 'symmetry', 'diagonal' and 'tubelane' vertical y~z planes[2], respectively.

Figure 7 depicts the same symmetry (vertical y~z) plane inlet and outlet side sludge thickness plots as in Figure 6 (for the CE System 80 Integral Economizer design), but with two additional horizontal x~y plane plots, at elevations approximately 20" above and below the uppermost partial tube support plate (09H in Figure 12).

Figures 8 through 11 depict the same calculated quantities as in Figures 4 through 7, respectively, at identical locations, for the CE Series 67 Non-Economizer design.

In Figures 4 through 11, it should be noted that:

- Velocities are colored by corresponding vapor fractions (which are scaled from 0 to 1).
- Sludge thicknesses are normalized from 0 to 1, indicating low potential (dark blue) to high potential (bright red), respectively. However, it may be of interest to know that (in all the sludge plots) the plotting scale was 'clipped' such that the red color indicates sludge thickness of: ≥ **4 mils**, which is what the Palo Verde investigators call 'thick' tube deposits.[5]
- To facilitate comparison with the Palo Verde data, Figures 4 and 8 include the axial locations and radial extent of the two partial tube support plates (08H and 09H in Figure 12) between which the tube rupture occurred.
- In the figures that have four vertical y~z plots, the two on the left are for the same (IX-) plane on the inlet/'hot' side and the two on the right are for the same (diametrically opposite IX-) plane on the outlet/'cold' side.
- In Figures 7 and 11, the lower of the two horizontal-plane sludge thickness plots is at the elevation of the center of the crack in the ruptured tube (Figure 12). The upper plot is centered on the area shown to have a large number of eddy-current indicators of potentially 'thick' deposits (in Figures 14 and 15).
- In the color plot titles, the CE System 80 and CE Series 67 steam generator designs are each referred to as Sample Steam Generators 1 and 2, respectively.

Observations

- The location of the leak (Figures 12 and 13) coincides **exactly** with a region of high potential for sludge deposition predicted by the model (Figures 5 and 7).
- In the vicinity of the leak, the utility found "thick ... bridging" sludge deposits (≥ 4 mils thick). The model predicts similarly thick deposits in this region.
- In both the SG21 and SG22 CE System 80 units at Palo Verde, eddy-current inspection readings indicated thick (above 2 to 5 mils deep) sludge deposits over a large area of tubes just above and just below the uppermost partial tube support plate, on the inlet/hot side (Figures 14 and 15). These sludge

---

[2] See Figure 3 for 'circumferential' plane definitions.

deposit indications appear to coincide **almost exactly** with two large regions of high potential for sludge deposition predicted by the model (Figures 4 through 7), in this same area.

- Various accounts of visual inspections of the leaking unit indicate that (on the hot side) up to about the 4th or 5th tube support plate, the tubes were relatively clean; but from there on up all the tubes were coated with a thin deposit layer that grew thicker and thicker until eventually they began to totally bridge the gap (between the tubes) by the time the area of the tube rupture was reached. This description seems to match well with the deposition patterns (if not the absolute thickness of the deposit) predicted by the sludge model in Figures 4 through 7.

- While investigating the tube rupture's cause, eddy-current inspections were also performed on a CE Series 67 non-economizer unit (at another site). This unit did not exhibit any indications of significant deposits in the region of the Palo Verde CE System 80 unit's failure. The sludge model is consistent with this behavior, predicting significantly lower likelihood for sludge deposition for the CE Series 67 (Figures 8 through 11) in the area of the System 80's ruptured tube.

- Interestingly, the eddy-current inspection data for SG21 (Figure 14) indicates a few thick sludge deposits on some vertical tube surfaces in the lower generator also. This too coincides with a small region of high sludge deposition potential predicted for the CE System 80 by the model (Figure 4).

Potential Impact of Technology

From these comparisons, with the limited amount of sludge deposition data available, it appears that mechanistically based models can accurately predict potentials for sludge at locations in a UTSG. With such capability, which has already been incorporated into ATHOS3 by EPRI, three dimensional CFD codes have the potential to be very valuable tools in helping to identify potential sludge 'trouble spots' **before** they introduce a corrosion concern. More importantly, these calculations provide the basis for more detailed local calculations of the chemical environment in and around support structures, under thick deposits, and within deep tubesheet sludge piles. Knowledge of the local chemical environment is essential to develop a mechanistic corrosion model for IGA/SCC, which can then be relied upon to optimize inspection and cleaning schedules and to facilitate the search for a fix.

CFD CALCULATION OF TEST THERMAL-HYDRAULICS

Background

Model Boiler Simulator Tests have been widely used in the power generation industry to study accelerated tube corrosion in secondary chemistries. To extrapolate the behavior in such tests to an operating heat exchanger, however, requires a thorough understanding of the local thermal-hydraulics.

To help acquire such an understanding, various CFD codes are available that could be adapted to analyze model boiler or simulator tests. To demonstrate the value that more sophisticated model boiler analysis capability could provide, the ATHOS3 steam generator thermal-hydraulic analysis program has been used to analyze a very simple, generic autoclave (boiling simulator) test bundle.

Case Considered

Figure 16 shows a generic boiling simulator bundle design that can be used to benchmark the rudimentary ATHOS3-based thermal-hydraulic calculation. The bundle is comprised of four SWAGELOK-elbow-connected vertical sections of heat transfer tubing, with each section having four simple **E**nhanced **C**oncentration **D**evices (ECDs) affixed in an alternating pattern (to prevent flow interference). Each ECD then serves as a 'flow-limiting chemistry concentrator', within which it is intended accelerated tube damage (functionally similar to tube/support plate crevice attack) will occur.

For illustration, the numerical simulation has been applied to three cases, covering a sample range of typical operating and geometry conditions:

1. A 'low' heat flux case, in a 3" diameter autoclave;
2. A 'high' heat flux case, in a 3" diameter autoclave; and
3. A 'high' heat flux case, in a 5" diameter autoclave.

Results Obtained

Examples of the calculated velocity and vapor fraction fields obtained for the three generic cases analyzed are shown in Figures 17 to 22. Some interesting points to note from these figures are as follows.

- The vector flow field for the low heat flux case (Figure 17) shows a fast-moving 'core' of vertical flow at the autoclave axis, a narrow 'pocket' of slow-moving downflow between the ECDs and boiler inner surface, large rotating 'eddies' above the top ECDs on the two 'short' tubes (i.e. the **non** inlet and outlet tubes), and a small pocket of basically stagnant liquid at the boiler bottom.

- The vector flow field for the 3" autoclave, high heat flux case (Figure 19) is **very different** from the corresponding low heat flux case, with: a slow-moving mix of upflow and downflow at the axis, a mix of faster-moving upflow and downflow between the ECDs and boiler inner surface, relatively small eddies above the top ECDs on the two shorter tubes and no longer stagnant liquid at the boiler bottom.

- The vector flow field for the 5"autoclave, high heat flux case (Figure 21) is, surprisingly, most similar to the 3"autoclave, low heat flux case, with: fast-moving vertical flow at the autoclave axis, a large recirculating eddy (in the gap between the ECDs and the boiler inner surface) extending from the water level down to the lowest ECDs and a large region of basically stagnant liquid at the boiler bottom.

- In all cases, the fastest-moving, (relatively) highest vapor fraction fluid is around the uppermost section of the inlet tube, where the highest heat fluxes are; the next fastest-moving, high vapor fraction fluid is around the uppermost section of the outlet tube, where the lowest heat fluxes are.

- Complex flow is apparent for all cases in the open tube sections between ECDs, with velocities and vapor fractions rising quickly here to then be deflected outward (by the next ECD bottom) to then mix (and 'quench') with the slower-moving and lower vapor fraction fluid flowing vertically past, just outside the plane of the ECDs.

- The low heat flux case shows much lower vapor fractions (Figure 16) throughout the autoclave and inside the ECDs vs. the two higher heat flux cases (Figures 18 and 20).

- o Pockets of higher vapor fraction can clearly be seen beneath all ECD bottoms, for all three cases studied (Figures 17, 19, 21).

The sludge deposition modeling capability discussed above for steam generator applications can be applied to a test vessel as well. An example of one such calculation is shown in Figure 23. This capability is valuable, since a complete laboratory mapping of corrosion must include sludge effects, which may vary depending upon the amount of sludge present locally.

Observations

From the results of the applications of the model described herein, several interesting 'gross' observations can be made on test bundle or ECD behavior, viz:

1. average heat fluxes within ECD 'wetted' regions (i.e. below the water level) are as much as 50% higher than calorimetric averages;

2. pressure drops across ECDs vary significantly throughout each model boiler;

3. the two most influential thermal-hydraulic parameters on individual ECD behavior appear to be heat flux and across-ECD pressure drop;

4. at like conditions, flow fields in model boilers with different diameters can be extremely dissimilar, yet produce ECD behavior that is very similar, depending upon ECD design; and

5. calculated ECD sludge buildup propensity shows considerable spatial variation, resulting from differences in local thermal-hydraulic variables such as heat flux and flow velocity.

Of course, the ultimate goal is to relate the 'global' (i.e. autoclave or heat exchanger) environment to the 'local' (i.e. ECD or crevice) environment so that relationships with corrosion can be derived. Toward this end, a 'concentration factor' can be calculated for each cell (control volume) used to represent the autoclave and ECD, based on the values of local thermal-hydraulic parameters. Results for one such calculation are shown in Figure 24. These results, in turn, can be used to calculate an ECD 'damage parameter' (= calculated concentration factor times liquid collapse level), as three-dimensionally plotted in Figure 25. From this surface plot, it is apparent that maximum ECD damage is predicted to occur with the highest tube-metal temperatures and lowest heat fluxes, which is consistent with a few data points obtained to benchmark calculations for this simple ECD geometry. The sensitivity of corrosion rate to thermal-hydraulic variables changes with the geometry of the ECD. Using this analytical capability, the ECD geometry (e.g., hole size and location) can be optimized to simulate specific conditions that have produced damage in the field.

Admittedly, this pseudo-local calculation is a gross simplification of the real case. The value of such calculations is that they allow the corrosion scientist to map the range of possible operating conditions to study general trends in local environmental variables known to affect corrosion. Similar calculations can be performed for the steam generator by extension of the technology demonstrated above. Armed with this knowledge, the researcher can design a test with conditions comparable to those expected in the field. These calculations also define the boundary conditions for more detailed local calculations of the environment inside the corrosion device (whether a generic ECD or a tube support plate). Definition of the local environment is required to develop mechanistic corrosion models that can be used to interpret test results and extrapolate to the plant application.

Potential Impact of Technology

The ability to characterize the thermal-hydraulic environment of heat exchanger crevices and test vessels is important if test results are to be extrapolated to improve field corrosion performance. Further development of this technology would allow optimization of test bundle design and loop operating conditions to be more prototypic of the local plant environment of interest. This would facilitate development of models to predict chemical concentration and material performance. The ability to run more focussed, prototypic tests may also allow a qualified fix (e.g. inhibitor or improved replacement design crevice configurations) to be developed more quickly.

CONCLUSION

An integrated investigative approach that merges technology from many diverse scientific disciplines is required to gain a fundamental understanding of corrosion, regardless of the mechanism. An important aspect of this integrated approach is characterization of the corrosive environment at high temperature, which begins with a thorough understanding of local thermal-hydraulic conditions. This paper has demonstrated the valuable role Computational Fluid Dynamics can play in characterizing the thermal-hydraulic environment, providing a basis to predict the consequences of that environment. With today's technology, accurate calculation of steam generator thermal-hydraulic conditions and the resulting sludge deposit profiles can be made, so that potential corrosion problems can be identified at an early stage and current corrosion problems can be better understood. With some code development, calculations are also possible for model boilers, so that tests can be designed to be prototypic of the heat exchanger environment they are supposed to simulate. Although progress is being made, continued emphasis on thermal-hydraulic technology is required to bridge the gap between laboratory and plant results and between the bulk and local environments. Continued development of CFD technology will facilitate development of models to predict chemical concentration and material performance, which will allow effective maintenance strategies to be developed and help focus the search for a fix.

REFERENCES

[1] L. W. Keeton, A. K. Singhal and G. S. Srikantiah, "ATHOS3: A Computer Program for Thermal-Hydraulic Analysis of Steam Generators", EPRI NP-4604-CCM, Volumes 1 to 3, July 1986.

[2] L. W. Keeton, R. H. Keefer, and P. R. Clark, "Integration of a Sludge Deposition Model into the ATHOS3 Computer Program and Application to a Sample U-Tube Steam Generator", Paper presented at EPRI Workshop on Secondary Side Initiated IGA/SCC, Minneapolis, MN, October 14-15, 1993.

[3] Keefer, R. H., Rider, J. L. and Waldman, L. A., "An Analytical Model for Particulate Deposition on Vertical Heat Transfer Surfaces in a Boiling Environment", in Proceedings of ADPA Predictive Technology Symposium, 1993, pp. 89-104.

[4] Singhal, A. K., Keeton, L. W., Przekwas, A. J. and Weems, J. S., "ATHOS: A Computer Program for Thermal-Hydraulic Analysis of Steam Generators", EPRI NP-2698-CCM, Volume 4, (Huntsville, Alabama: CHAM of North America, Inc., 1984).

[5] Sweeney, K. and Melton, M., "Free-Span IGA/SCC at the Palo Verde Nuclear Generating Station", Paper Presented by Arizona Public Service Company at EPRI IGA/SCC Workshop, Minneapolis, Minnesota, October 14-15, 1993.

CE SYSTEM 80 STEAM GENERATOR

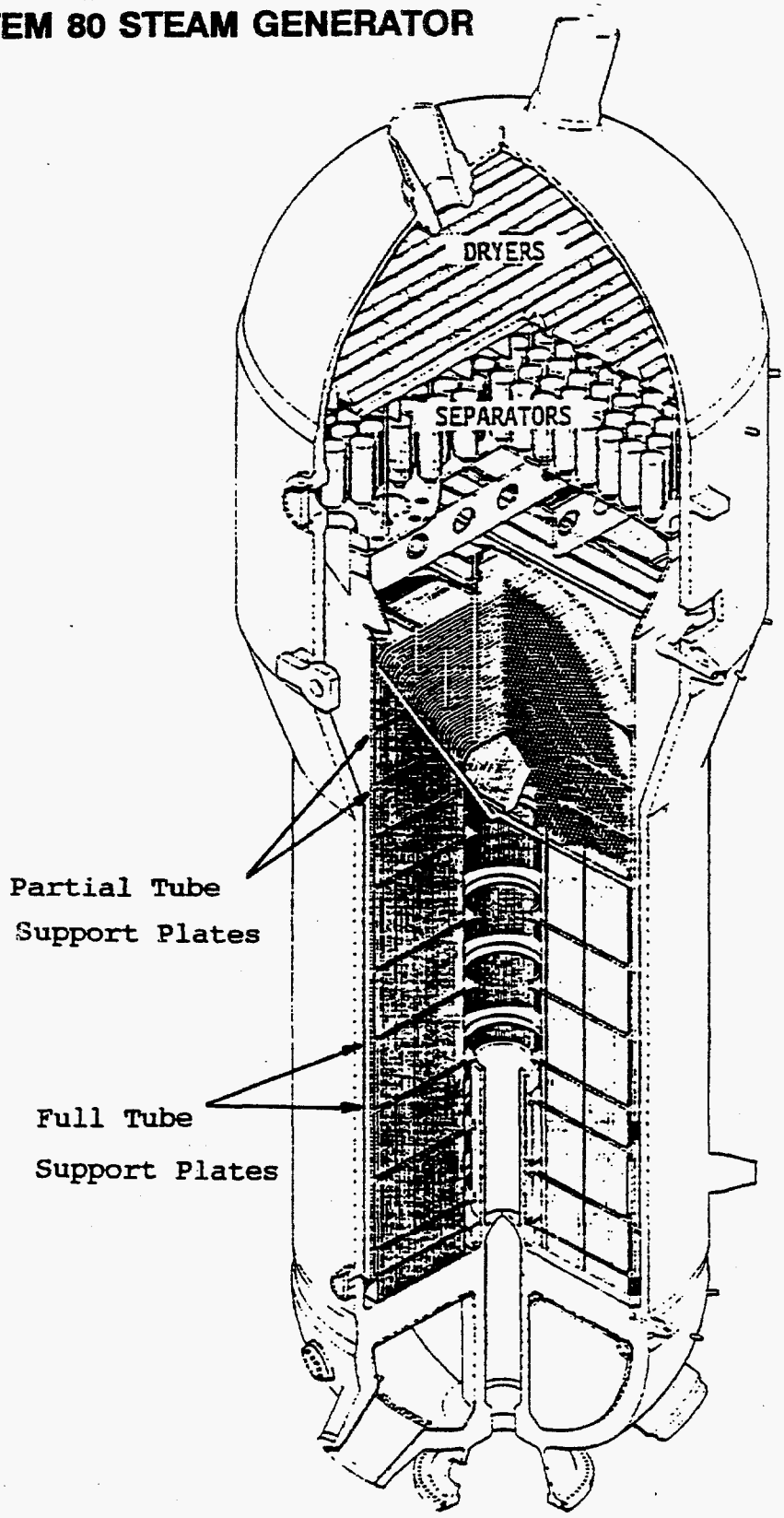

Figure 1. CE System 80 Steam Generator.

CE SERIES 67 STEAM GENERATOR

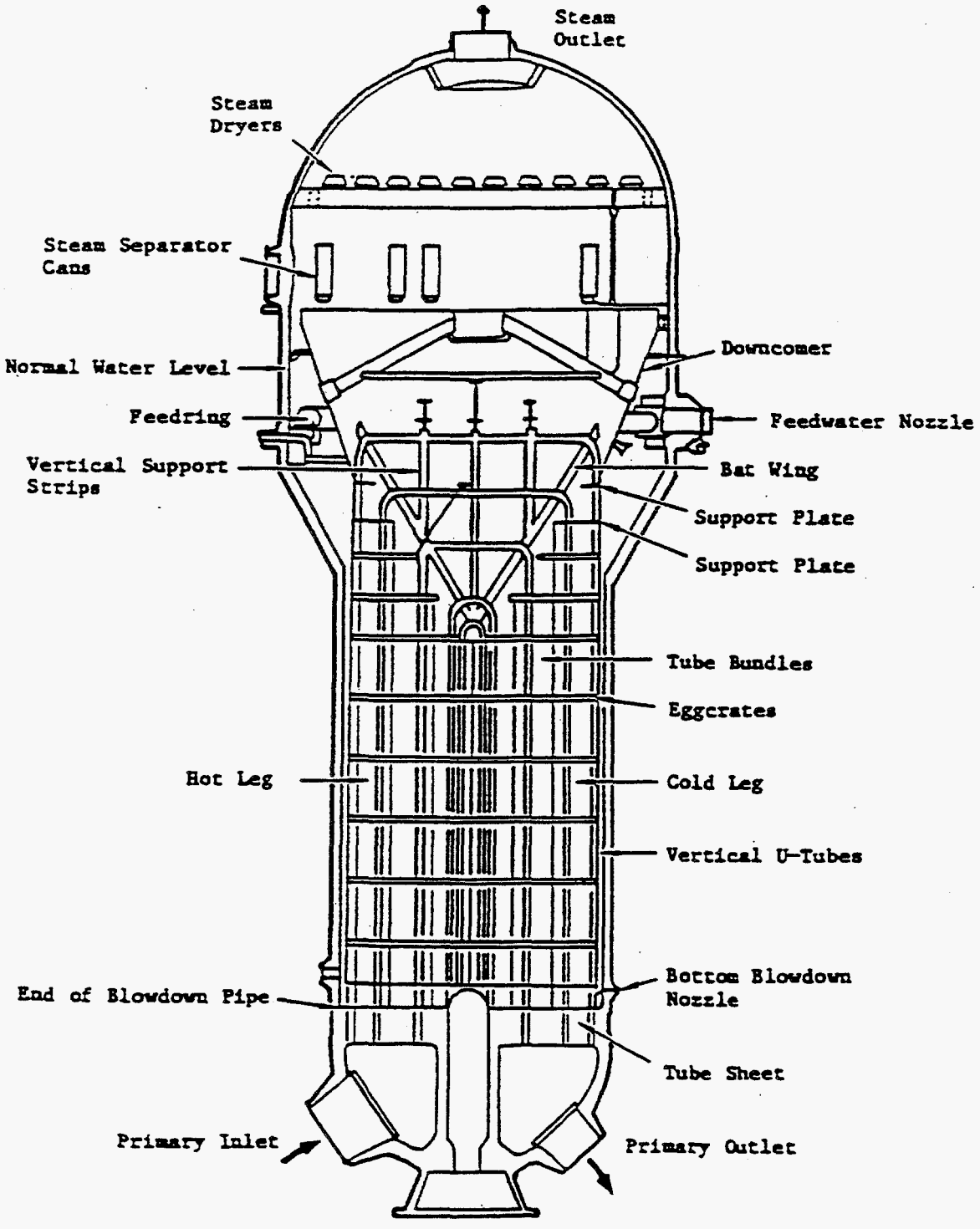

Figure 2. CE Series 67 Steam Generator.

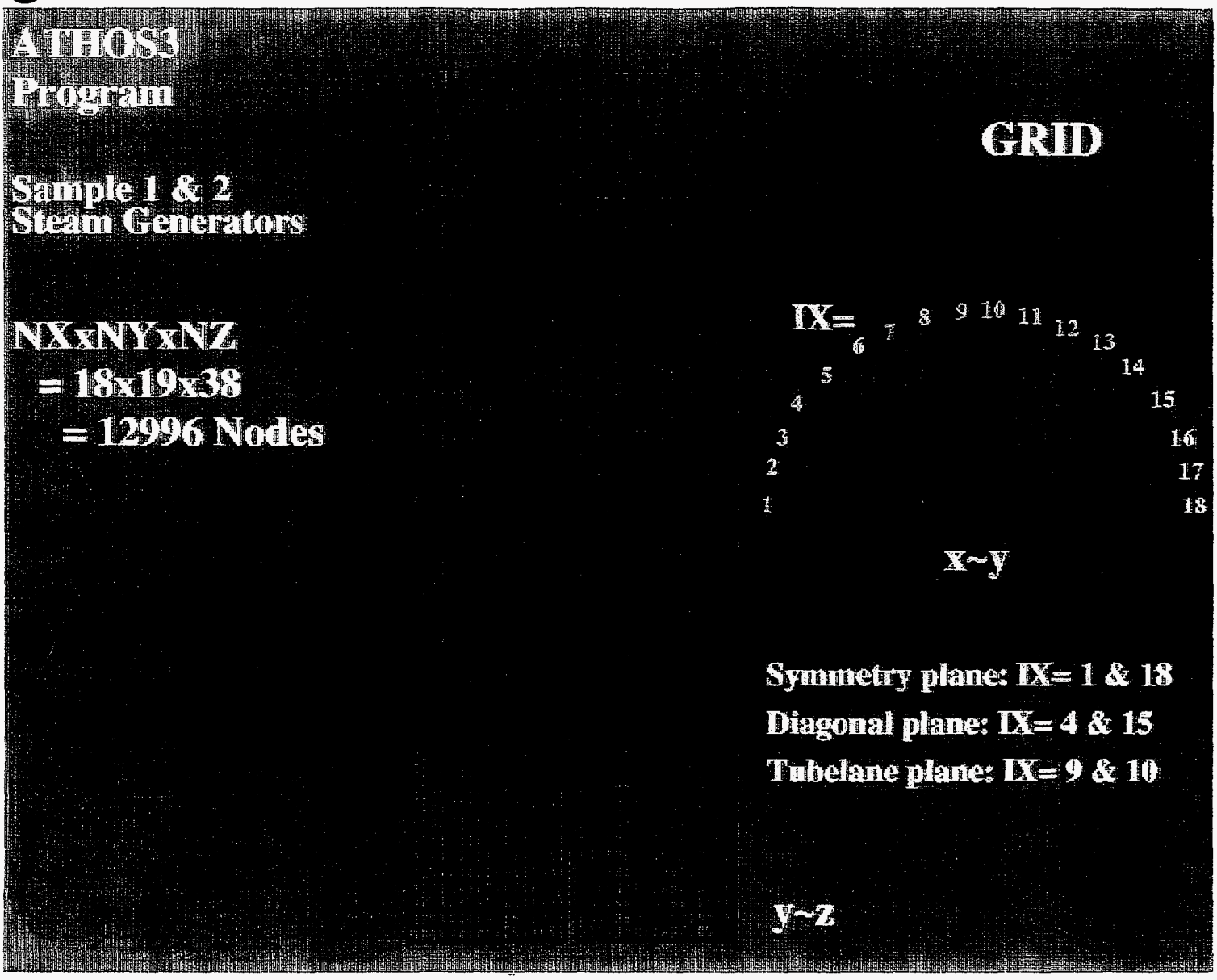

Figure 3. Computational Grid For CE System 80 and Series 67 Numerical Models.

In Figures 3 through 11:

Sample 1 Steam Generator = CE System 80

Sample 2 Steam Generator = CE Series 67

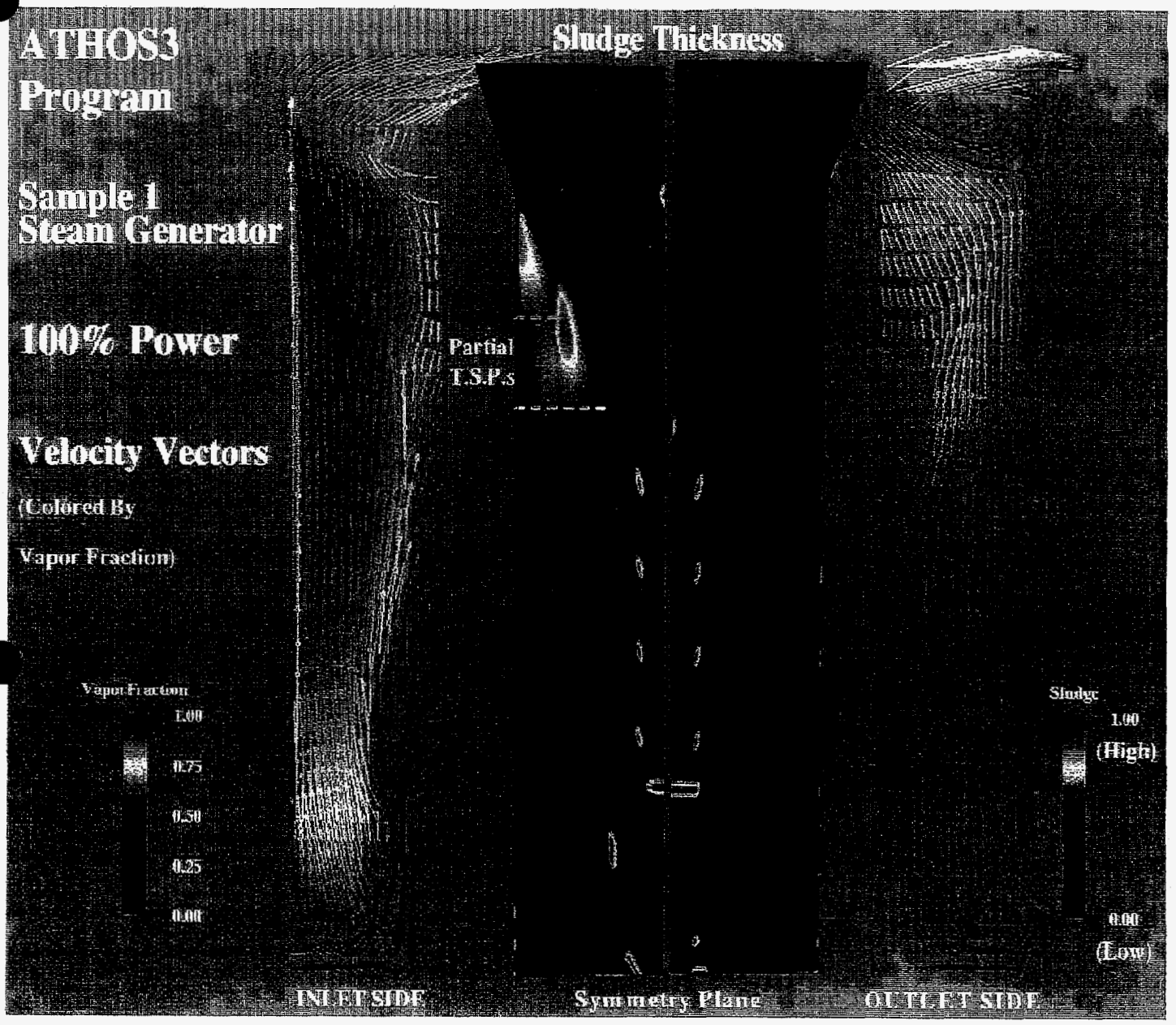

Figure 4. Calculated CE System 80 Velocity Vectors and Sludge Deposits at Symmetry Plane.

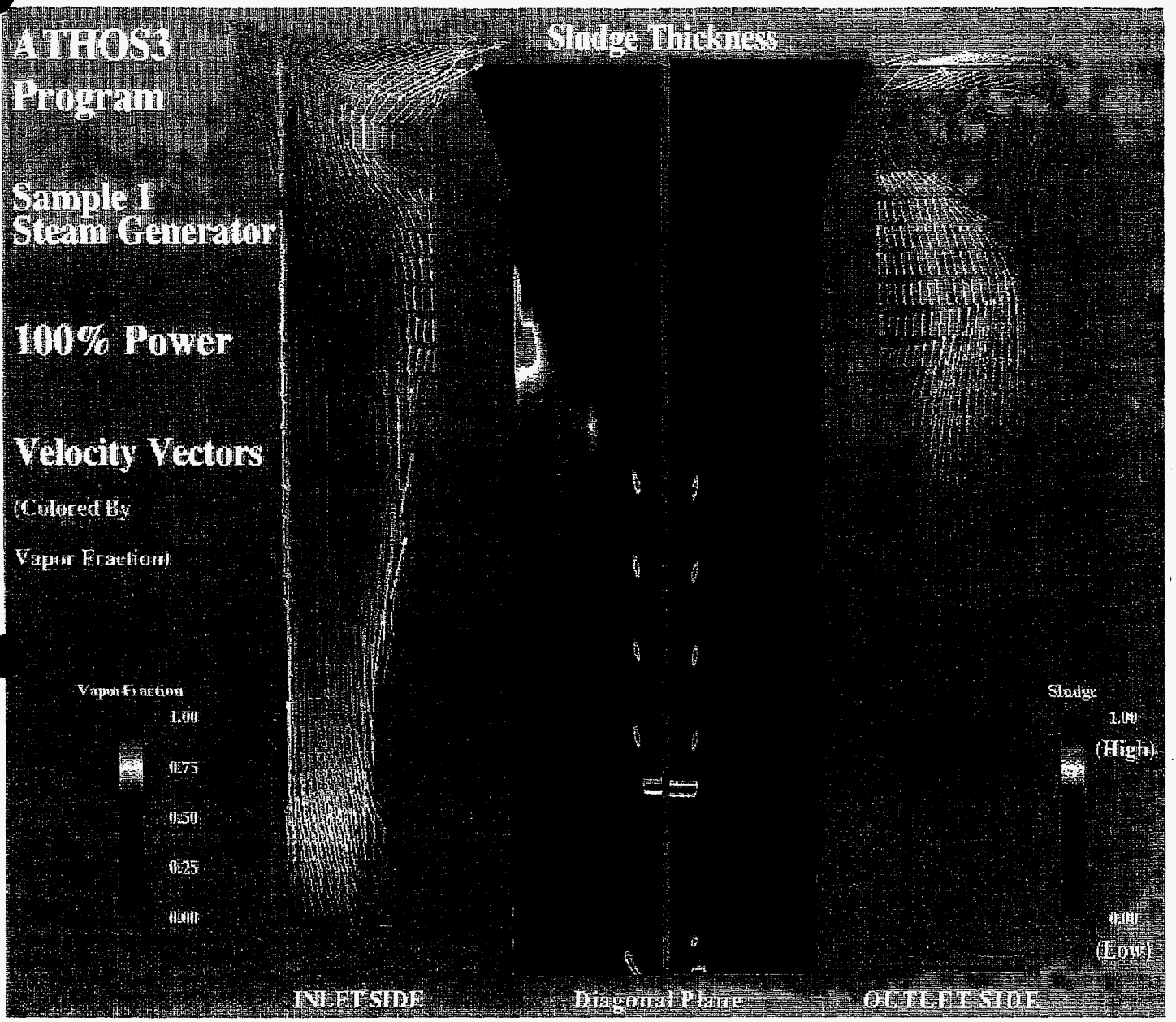

Figure 5. Calculated CE System 80 Velocity Vectors and Sludge Deposits at Diagonal Plane.

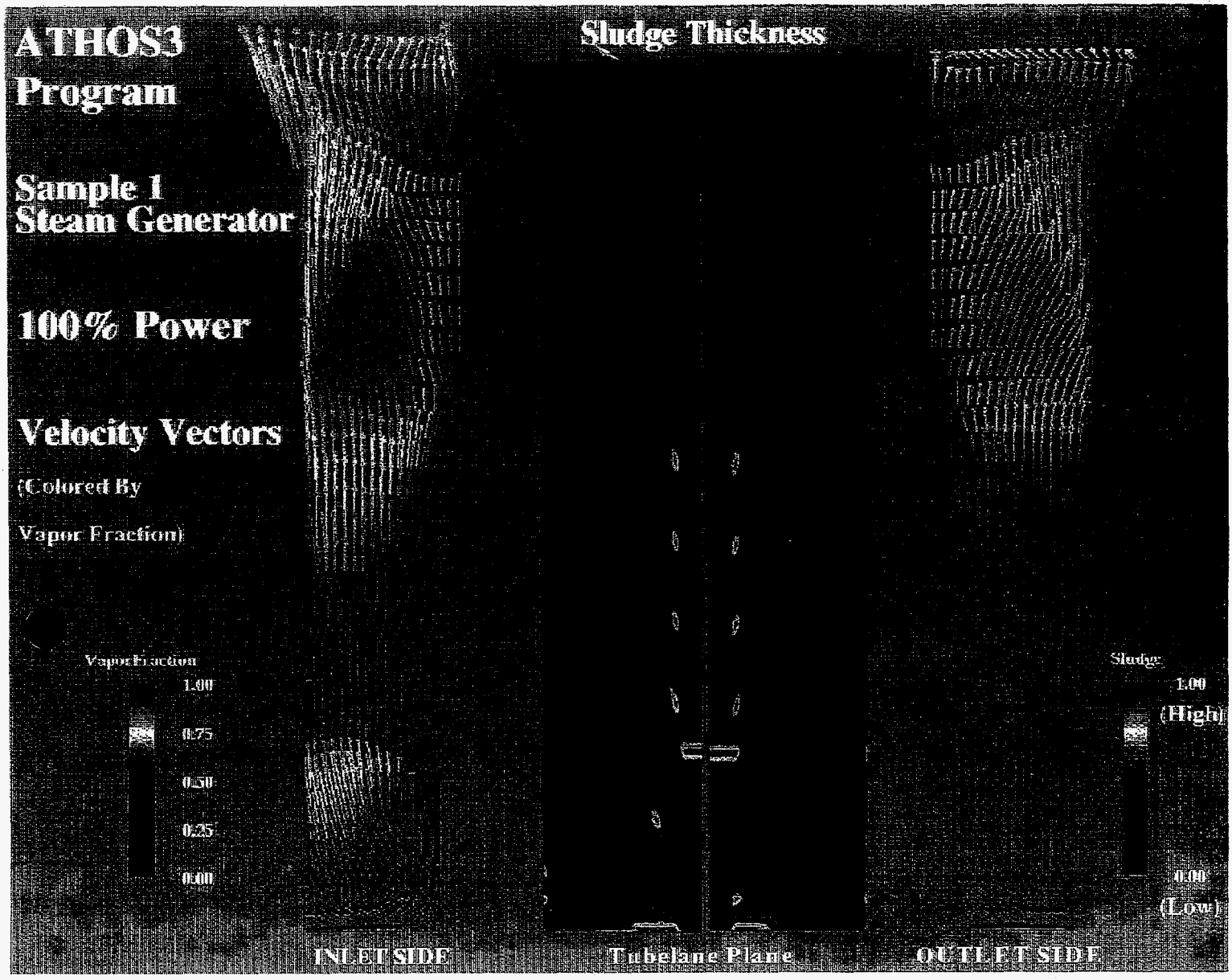

Figure 6. Calculated CE System 80 Velocity Vectors and Sludge Deposits at Tubelane Plane.

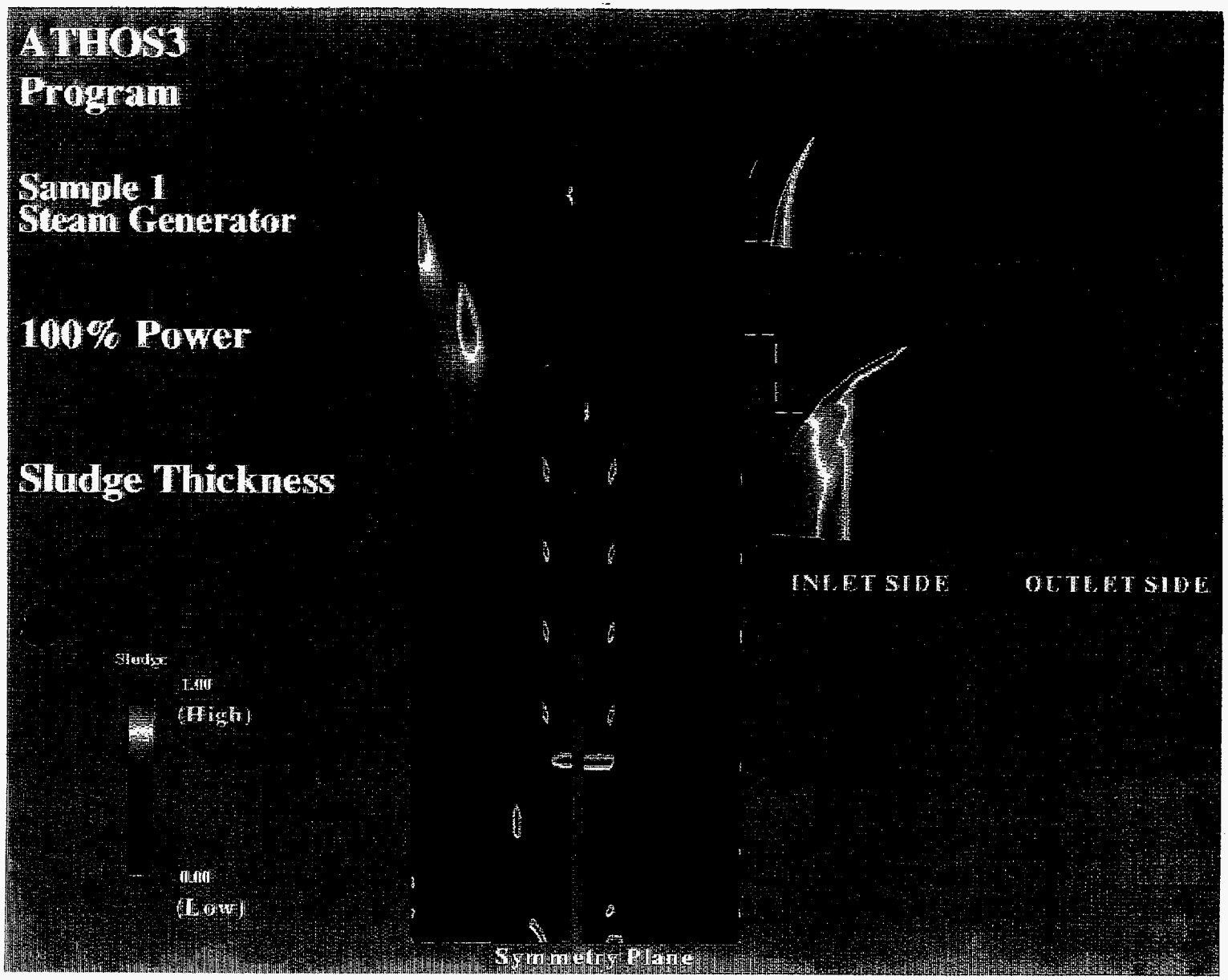

Figure 7. Calculated CE System 80 Velocity Vectors and Sludge Deposits Near 09H Support Plate.

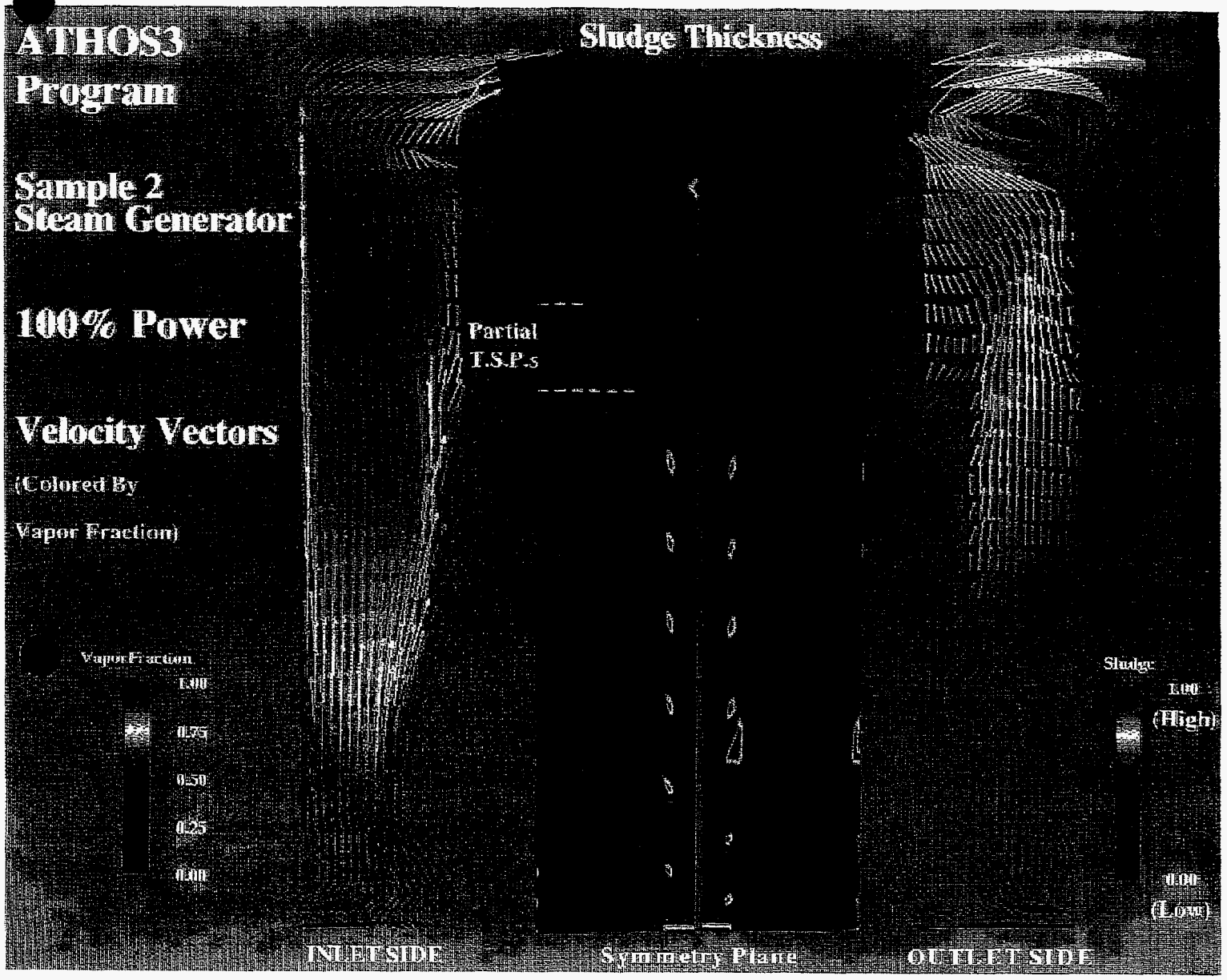

Figure 8. Calculated CE Series 67 Velocity Vectors and Sludge Deposits at Symmetry Plane.

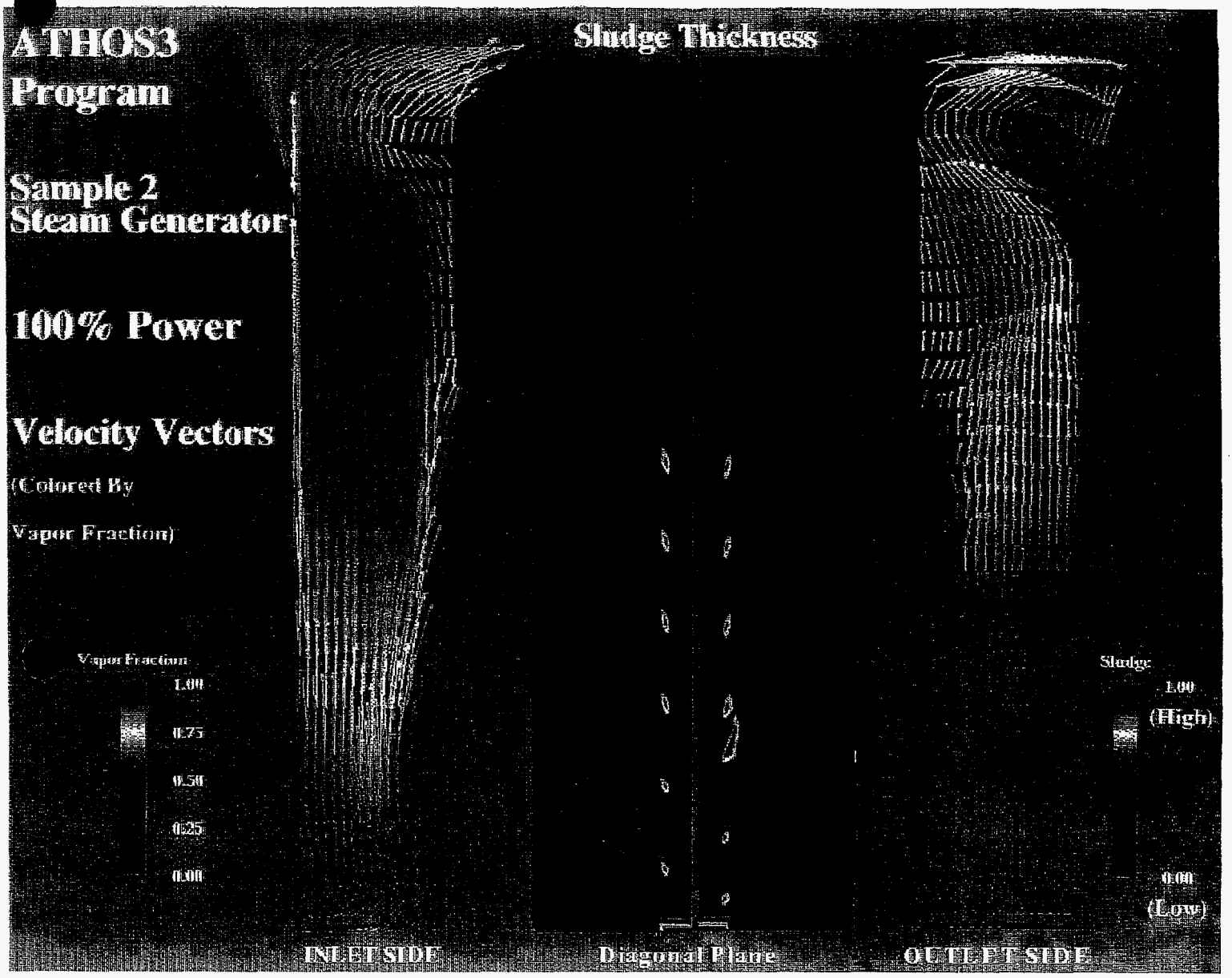

Figure 9. Calculated CE Series 67 Velocity Vectors and Sludge Deposits at Diagonal Plane.

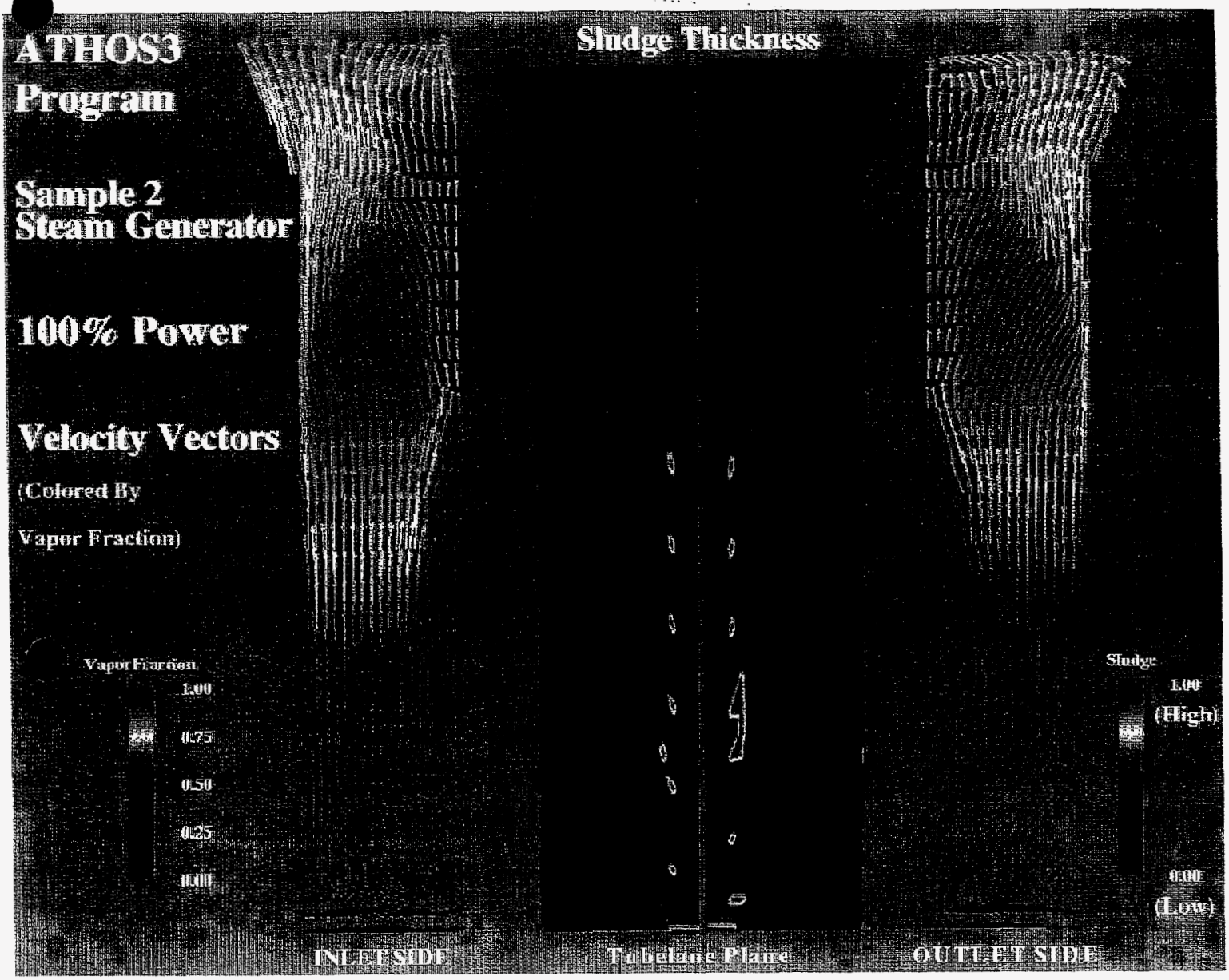

Figure 10. Calculated CE Series 67 Velocity Vectors and Sludge Deposits at Tubelane Plane.

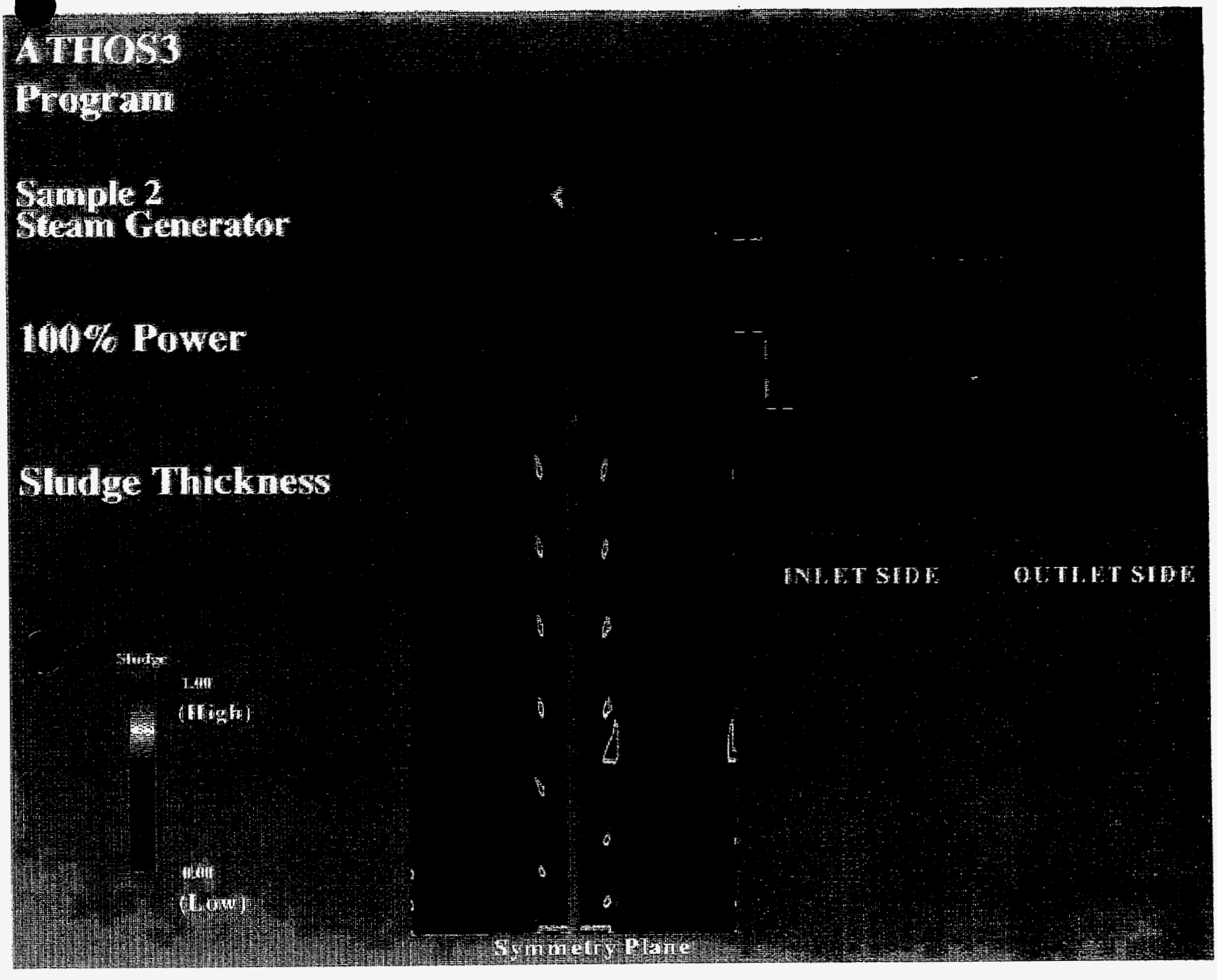

Figure 11. Calculated CE Series 67 Velocity Vectors and Sludge Deposits Near 09H Support Plate.

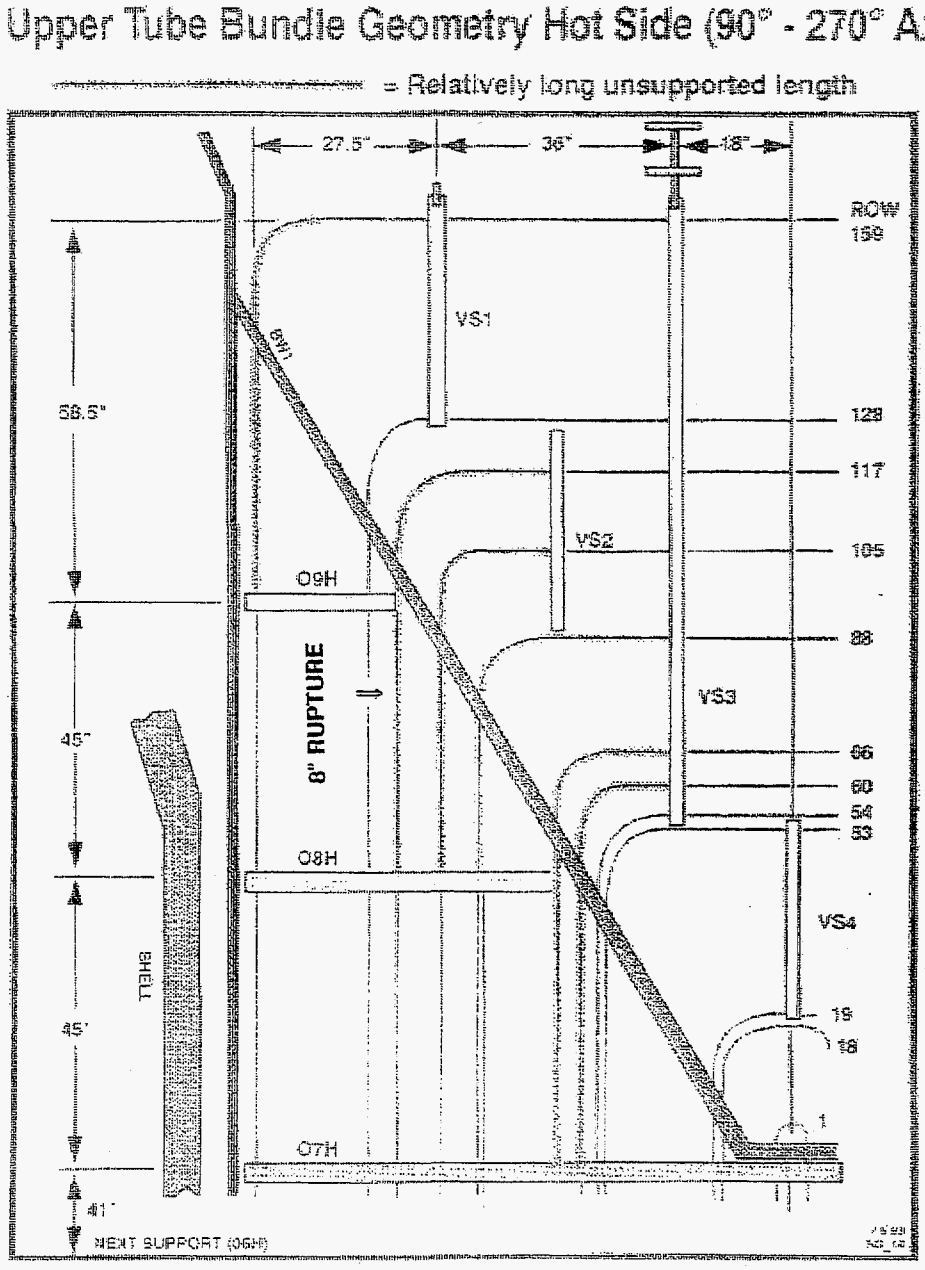

Figure 12. Palo Verde CE System 80 Tube Rupture Location, Vertical Plane.

Figure reproduced from Reference 5.

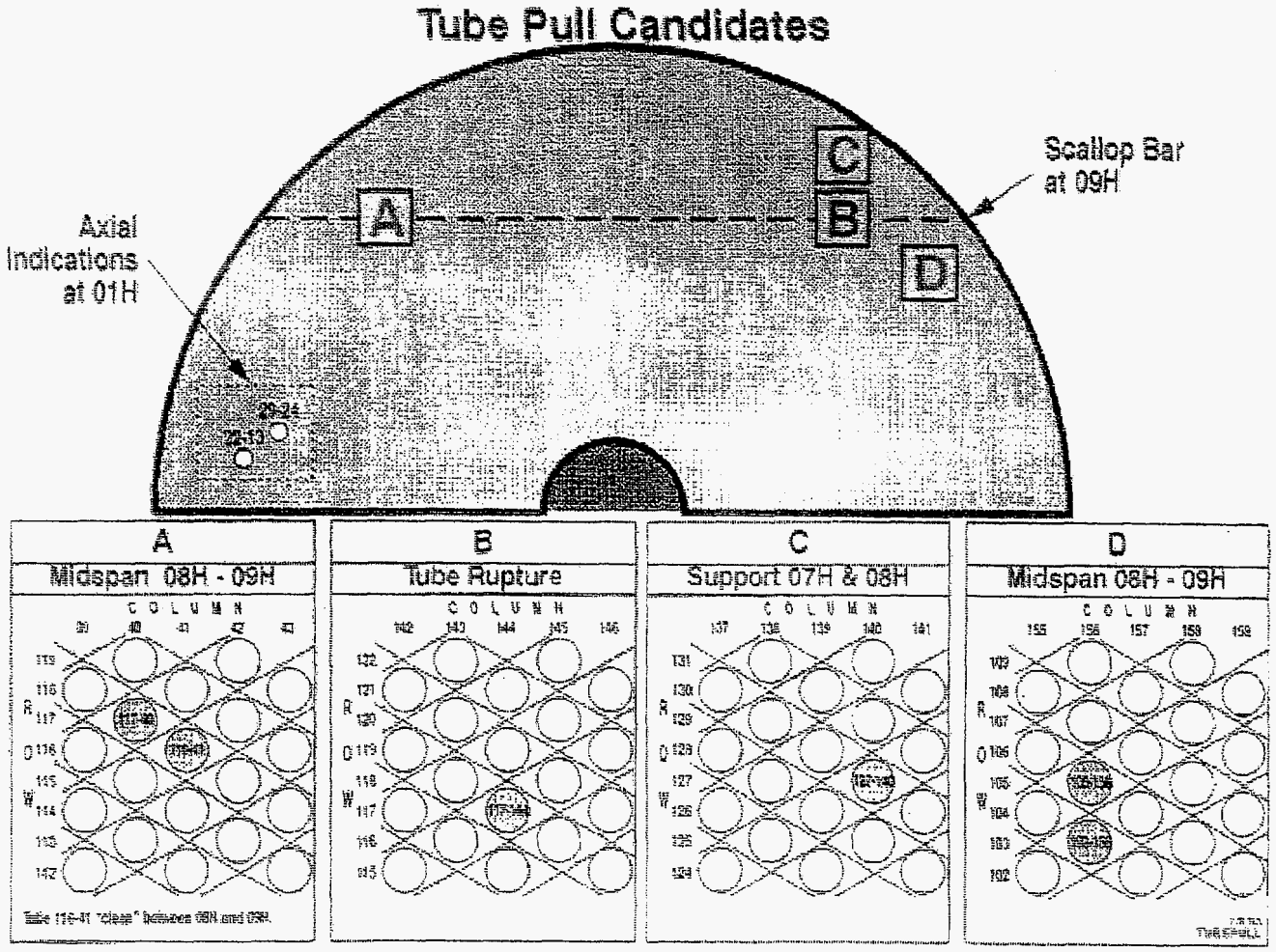

Figure 13. Palo Verde CE System 80 Tube Rupture Location, Horizontal Plane.

Figure reproduced from Reference 5.

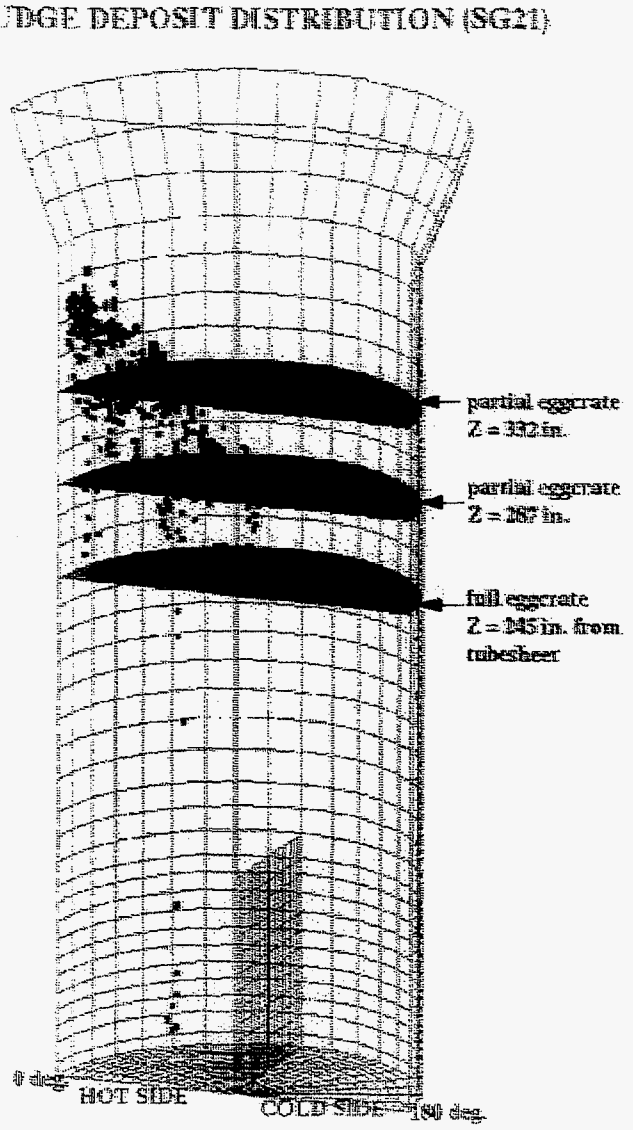

Figure 14. Sludge Deposit Distribution in Palo Verde CE System 80 Unit SG21.

Figure supplied by EPRI.

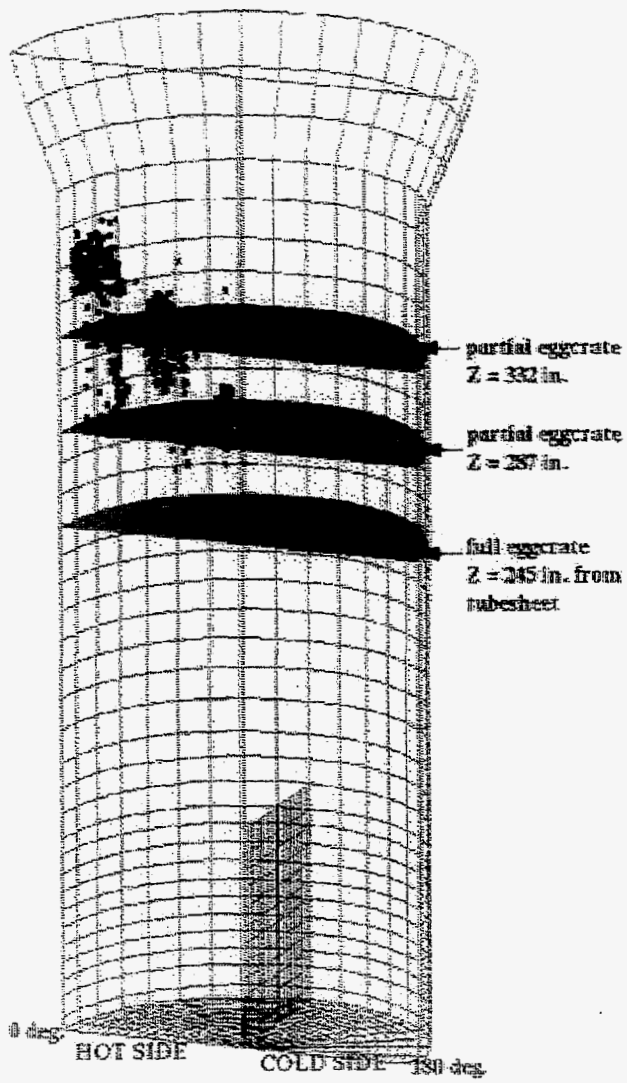

Figure 15. Sludge Deposit Distribution in Palo Verde CE System 80 Unit SG22.

Figure supplied by EPRI.

MODEL BOILER SIMULATOR TEST BUNDLE

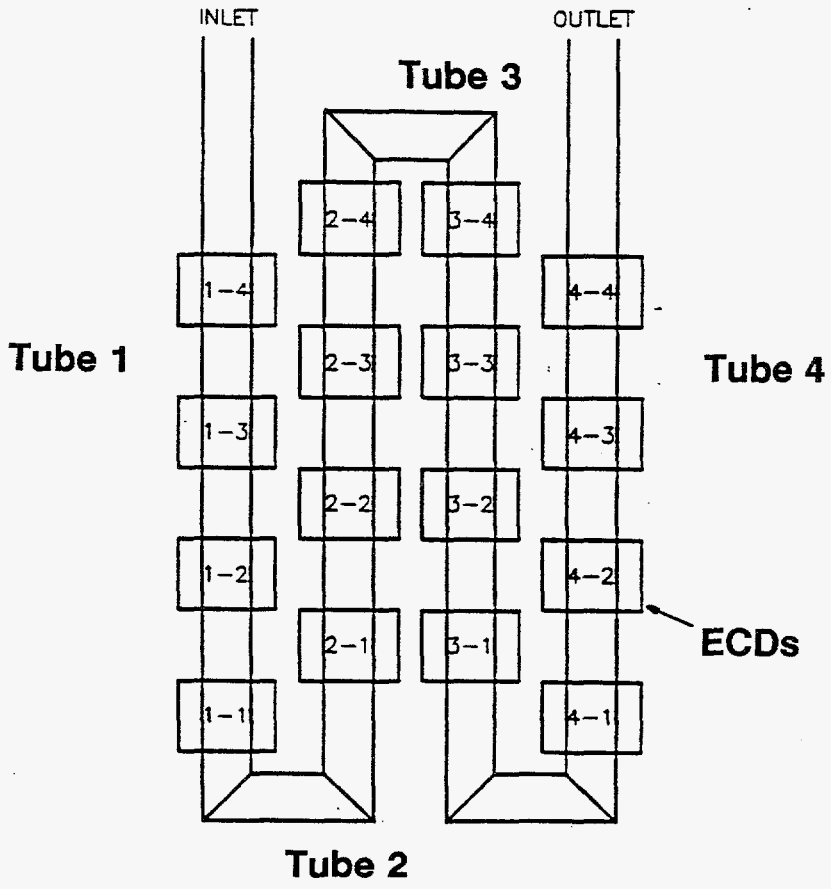

ENHANCED CONCENTRATION DEVICE

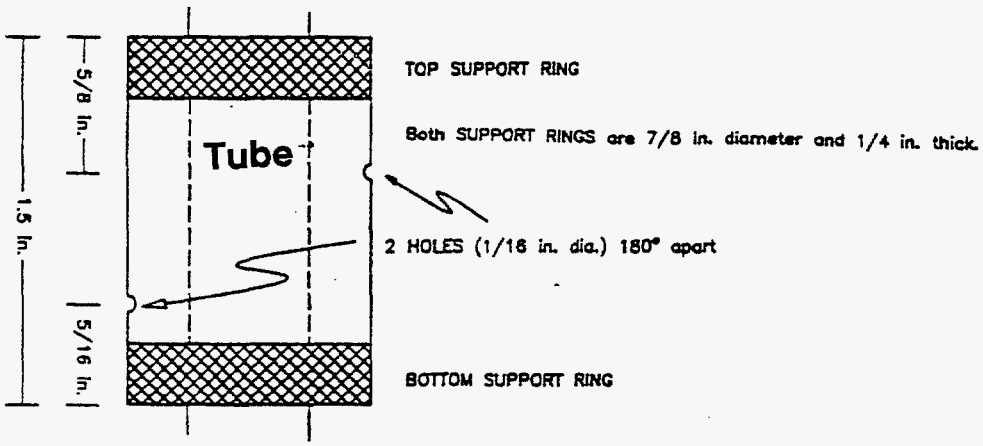

Figure 16. Model Boiler Simulator Test Bundle and ECD Design.

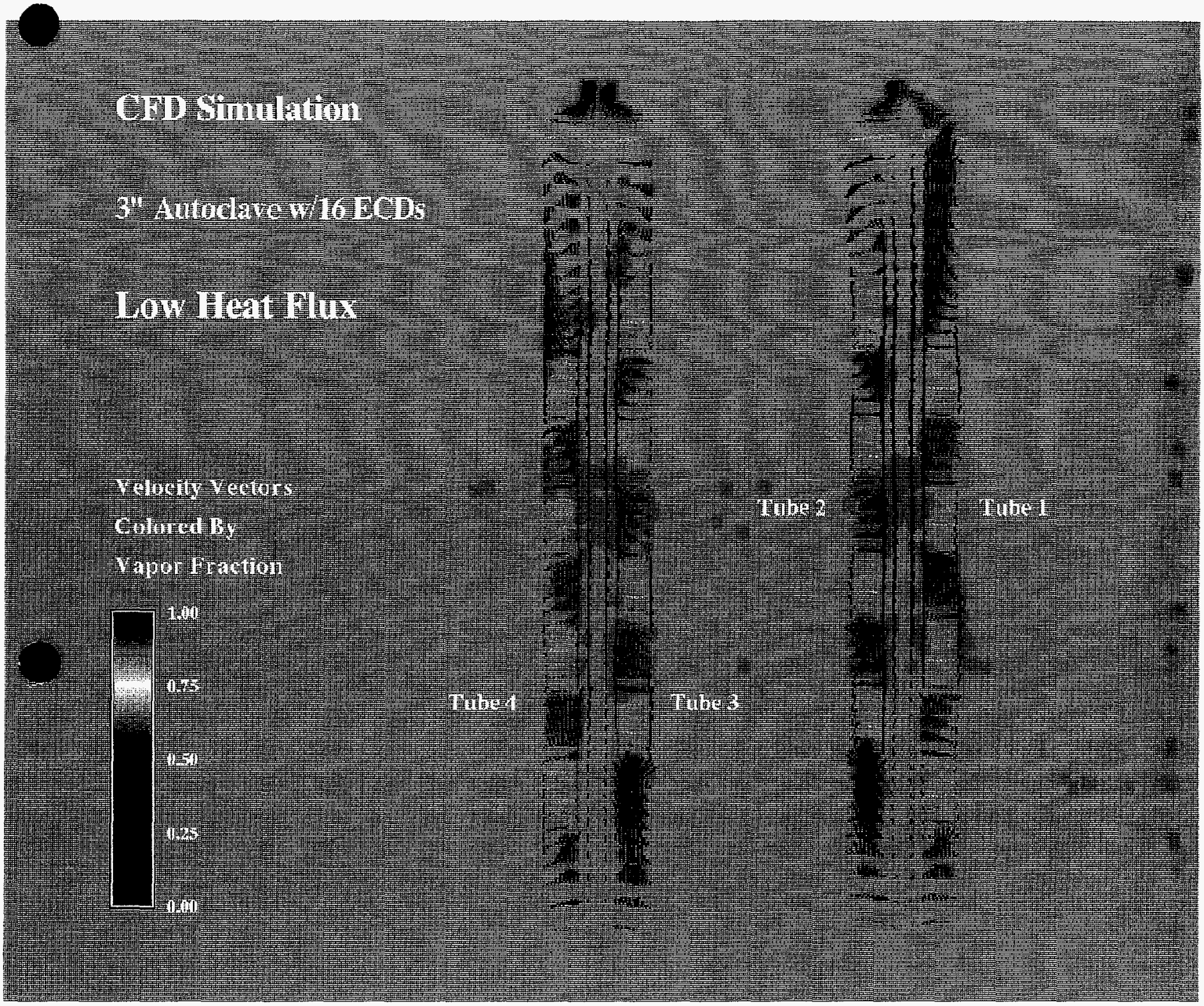

Figure 17. Calculated Velocity Vectors for 3" Autoclave, With Low Heat Flux.

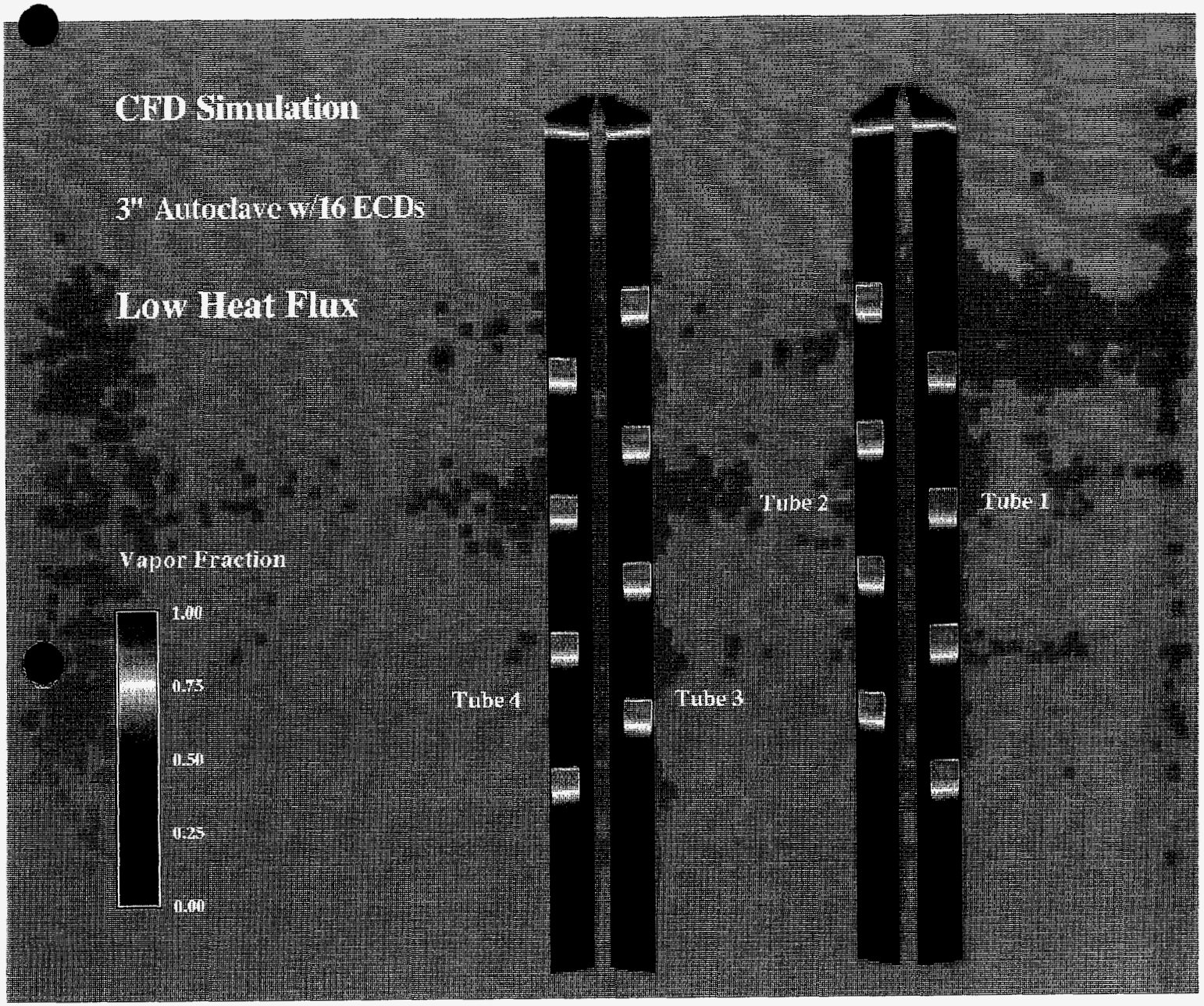

Figure 18. Calculated Vapor Fractions for 3" Autoclave, With Low Heat Flux.

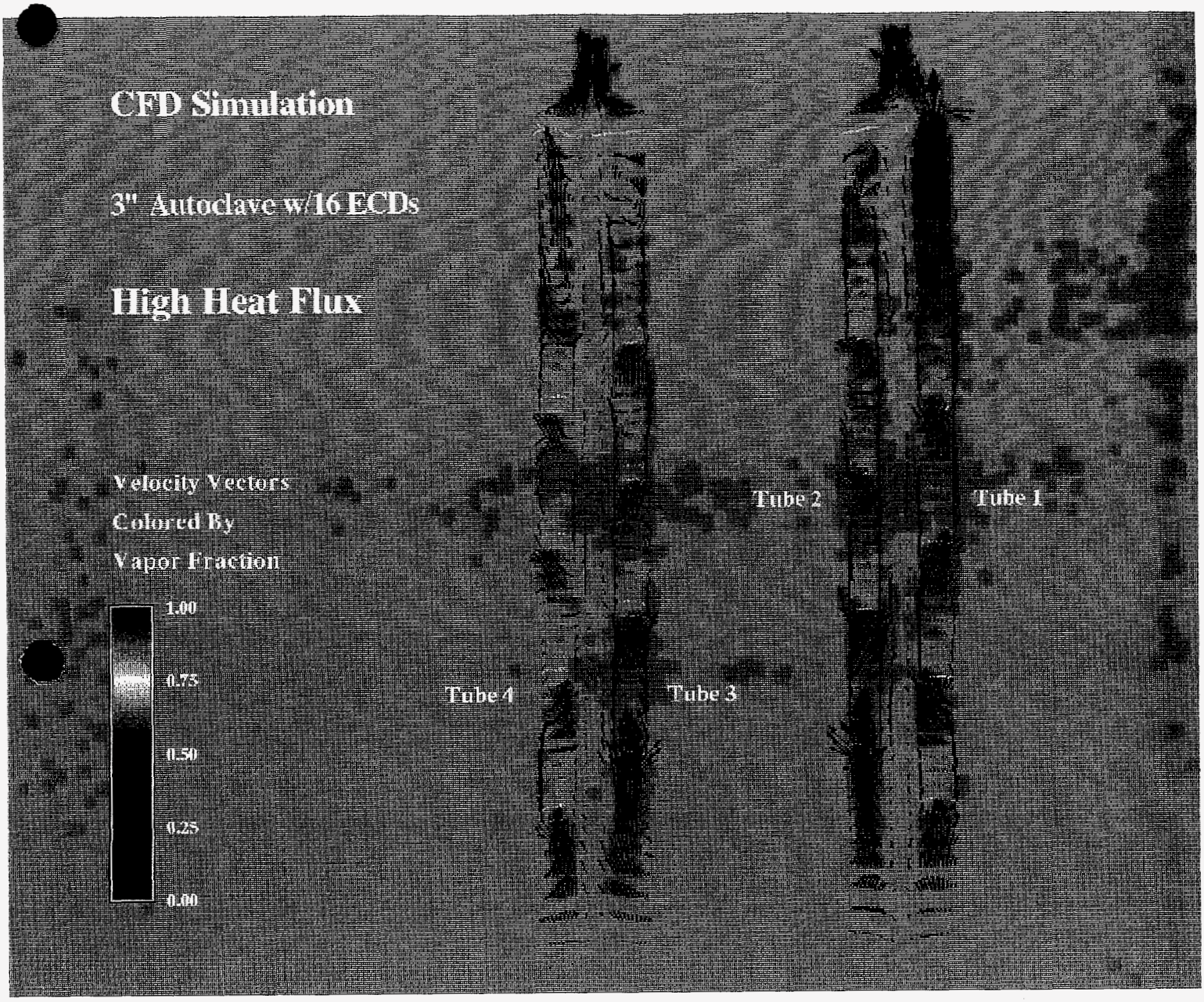

Figure 19. Calculated Velocity Vectors for 3" Autoclave, With High Heat Flux.

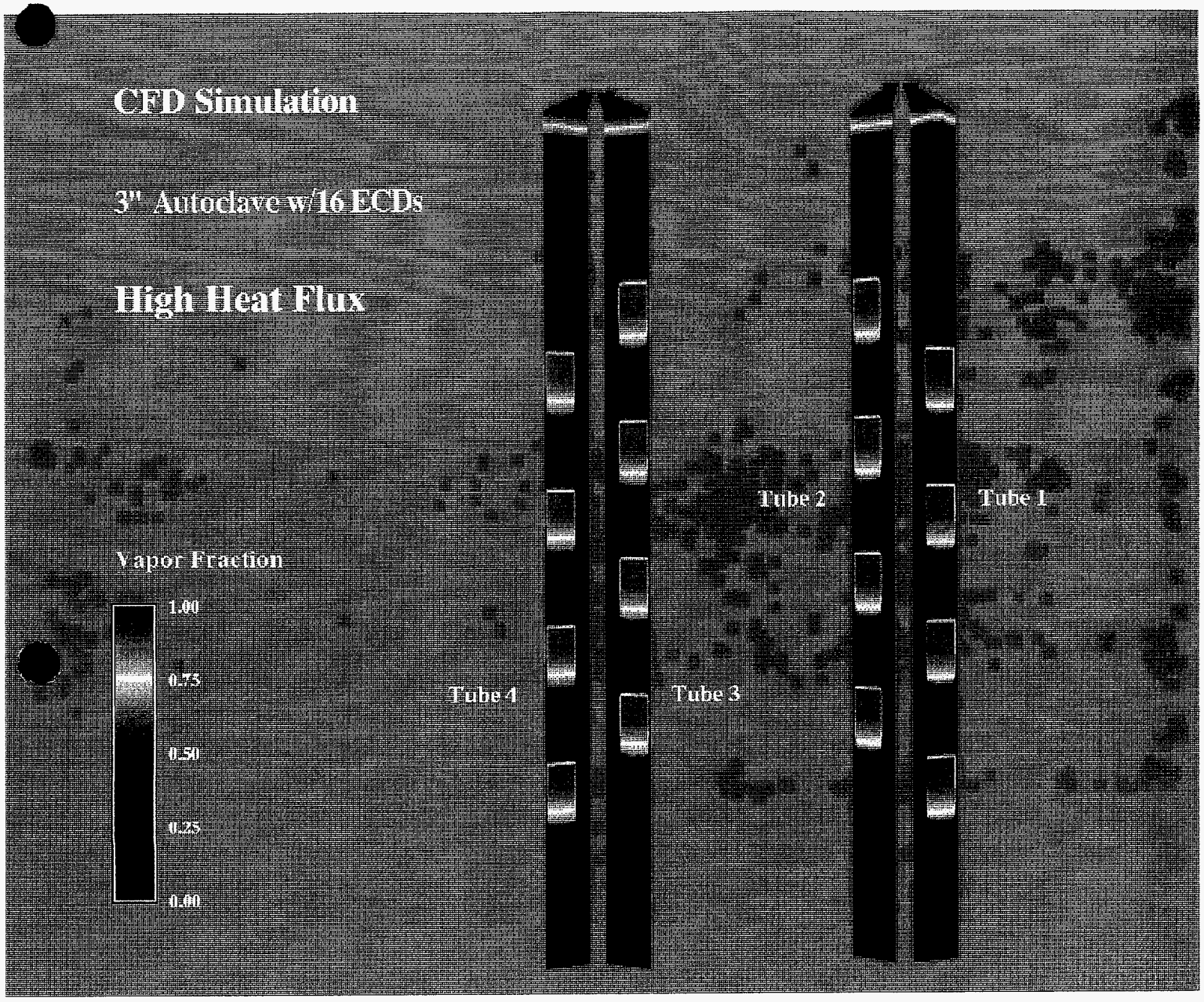

Figure 20. Calculated Vapor Fractions for 3" Autoclave, With High Heat Flux.

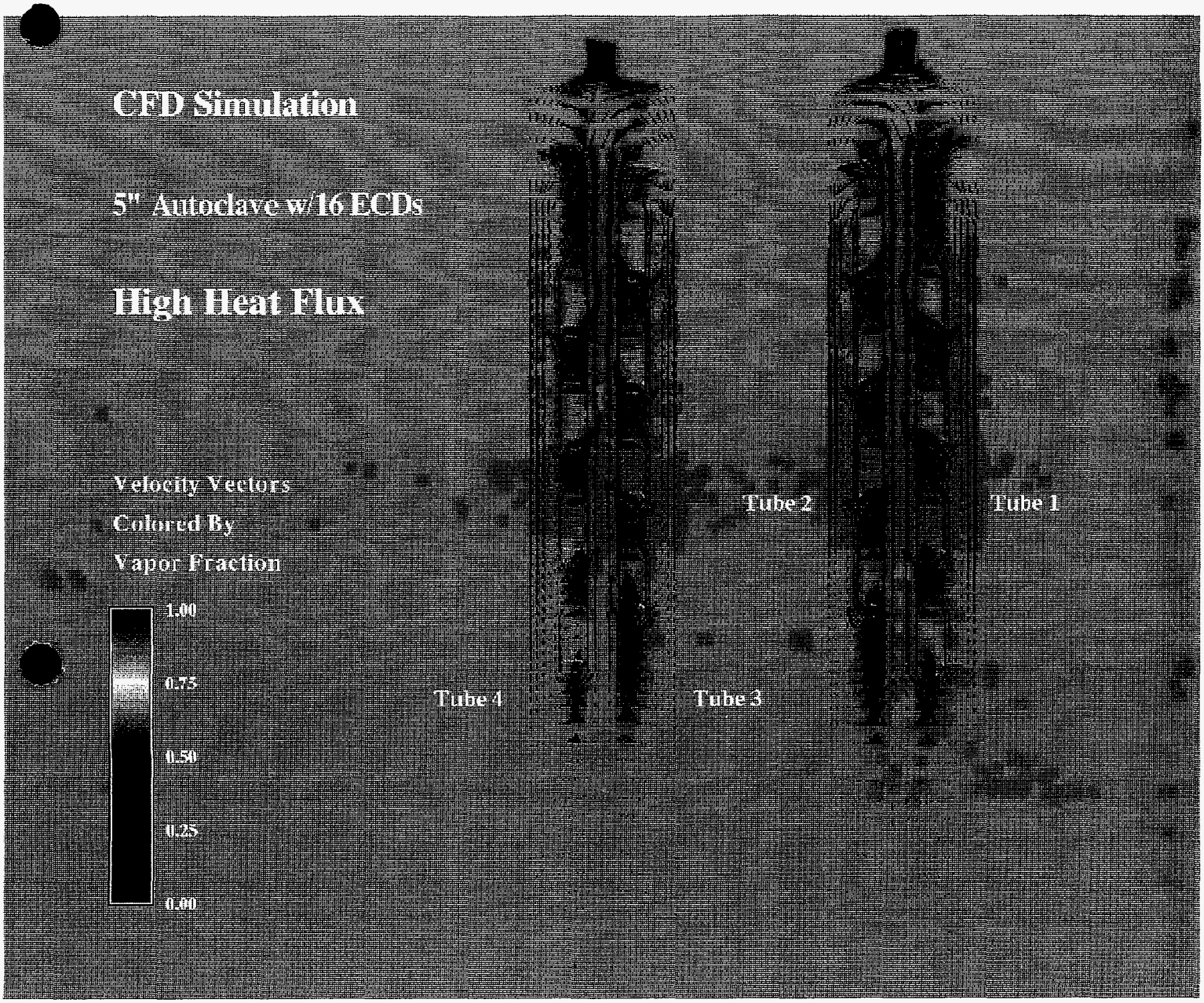

Figure 21. Calculated Velocity Vectors for 5" Autoclave, With High Heat Flux.

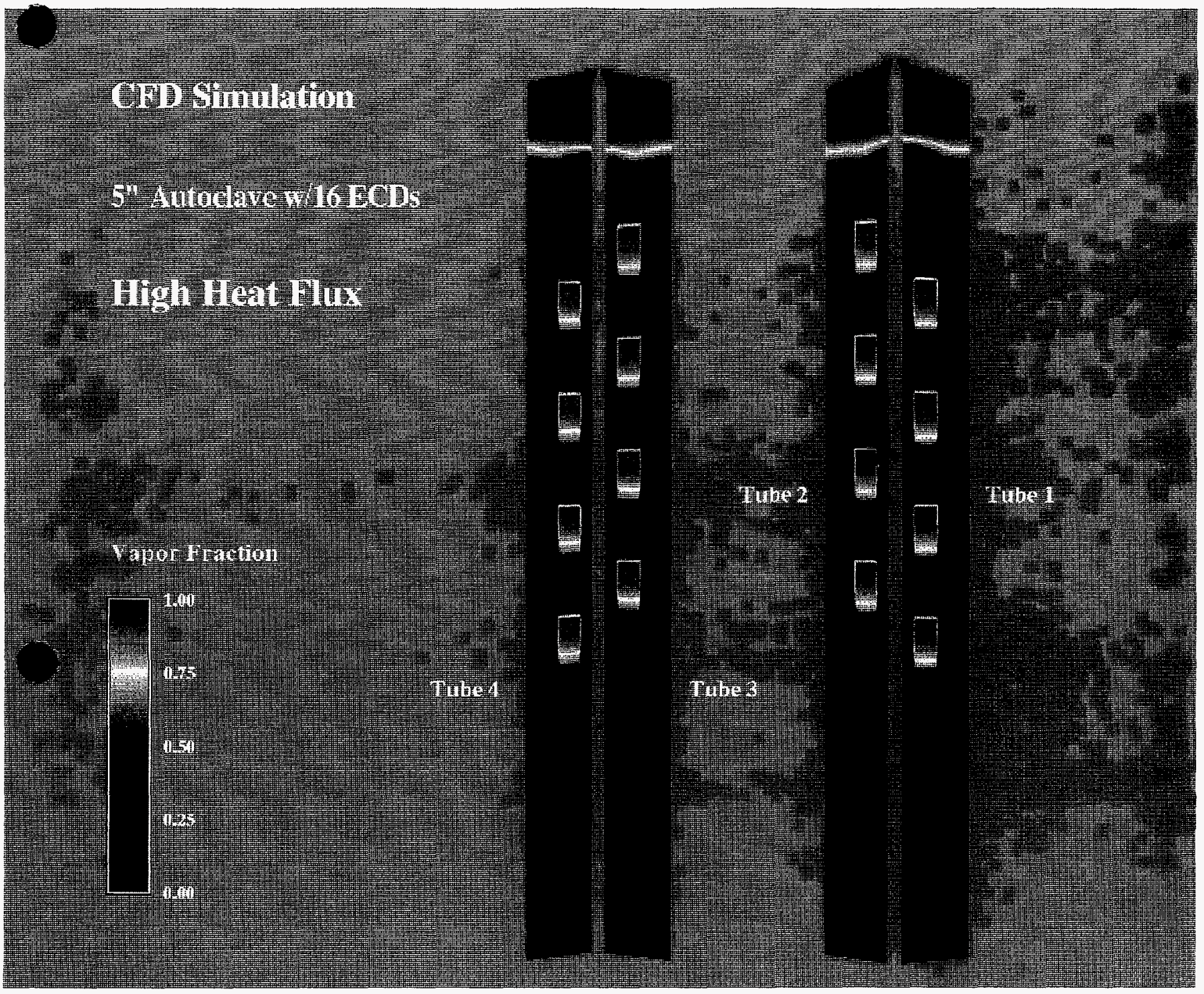

Figure 22. Calculated Vapor Fractions for 5" Autoclave, With High Heat Flux.

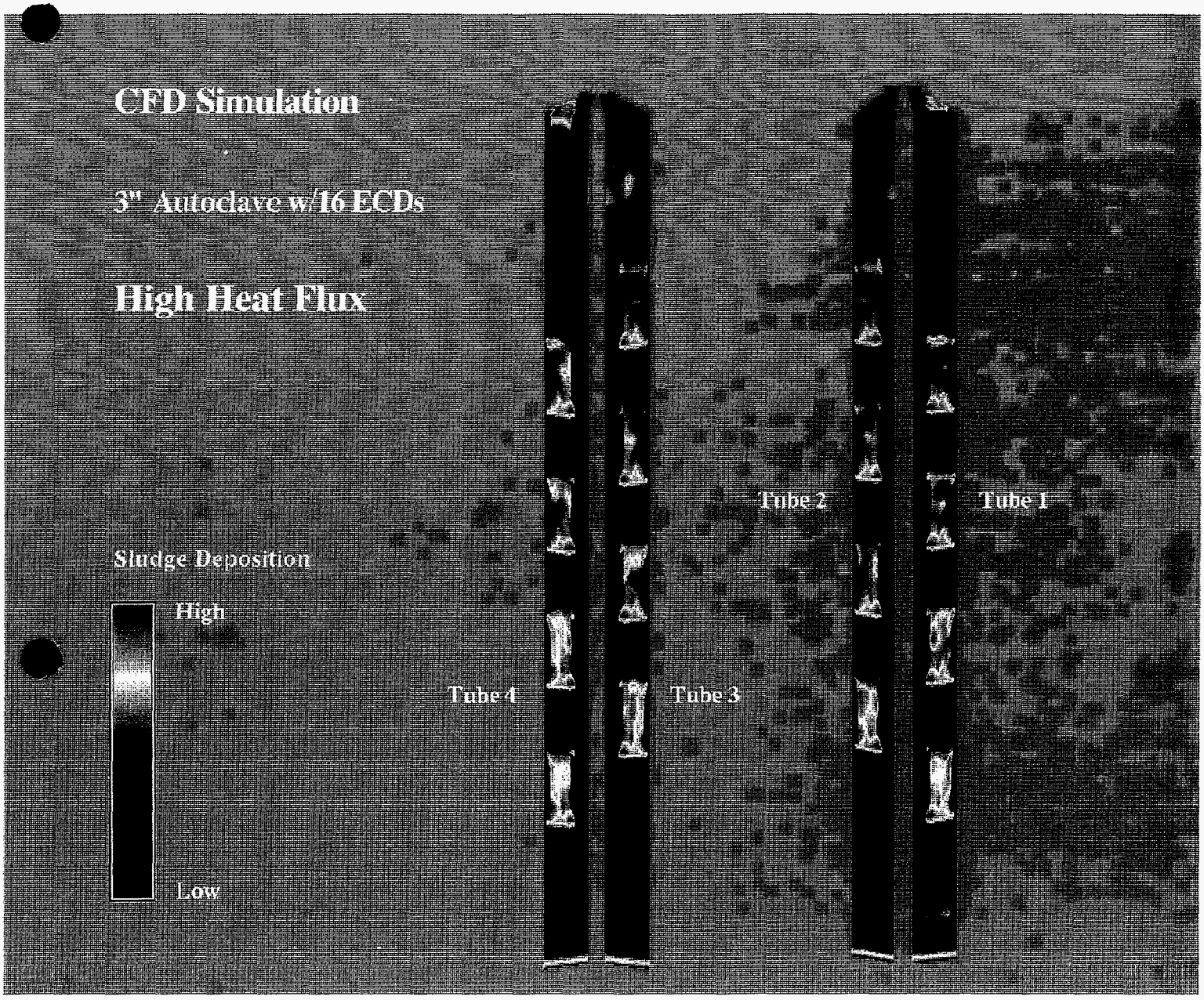

Figure 23. Calculated Sludge Deposits for 3" Autoclave, With High Heat Flux.

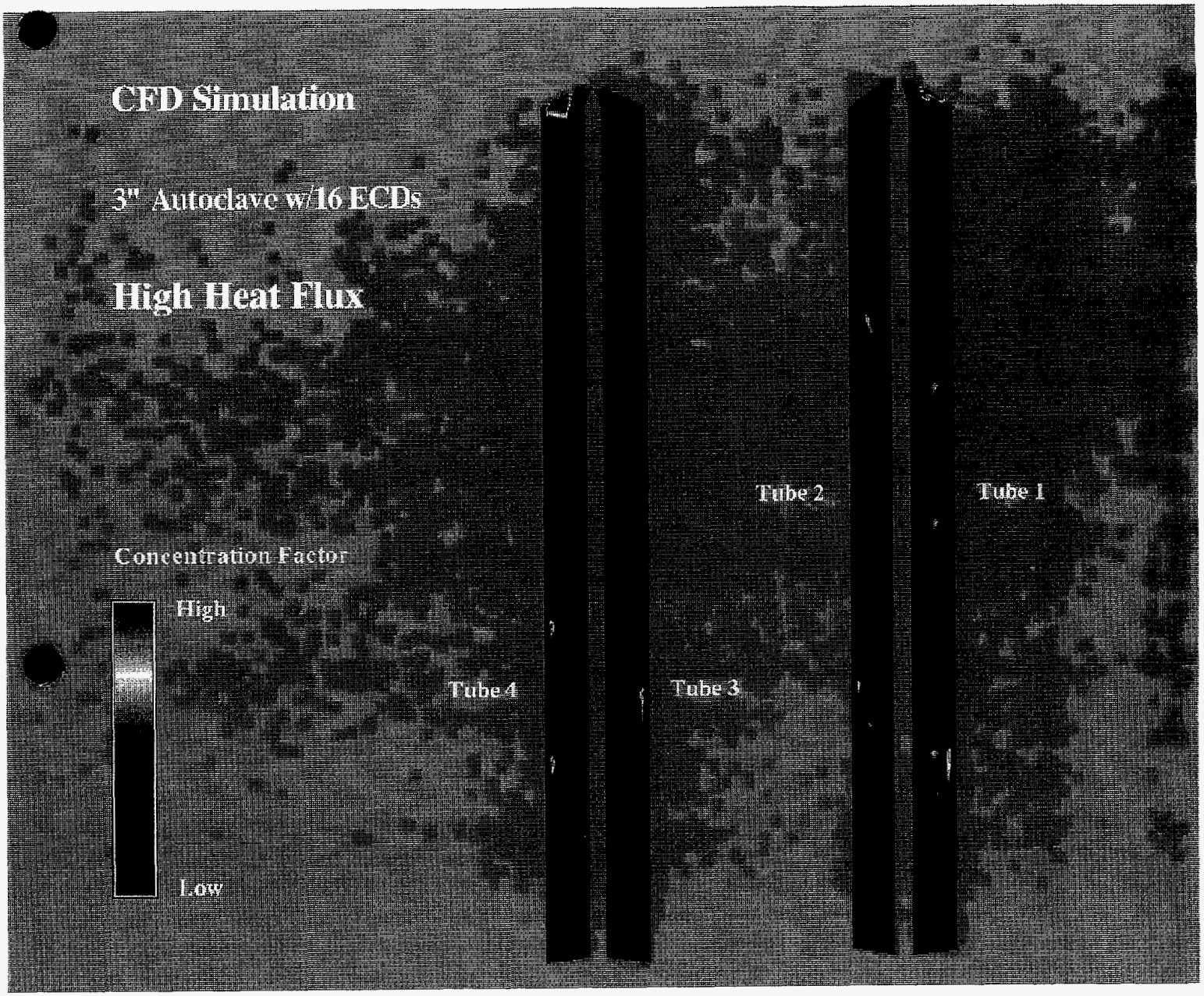

Figure 24. Calculated Concentration Factors for 3" Autoclave, With High Heat Flux.

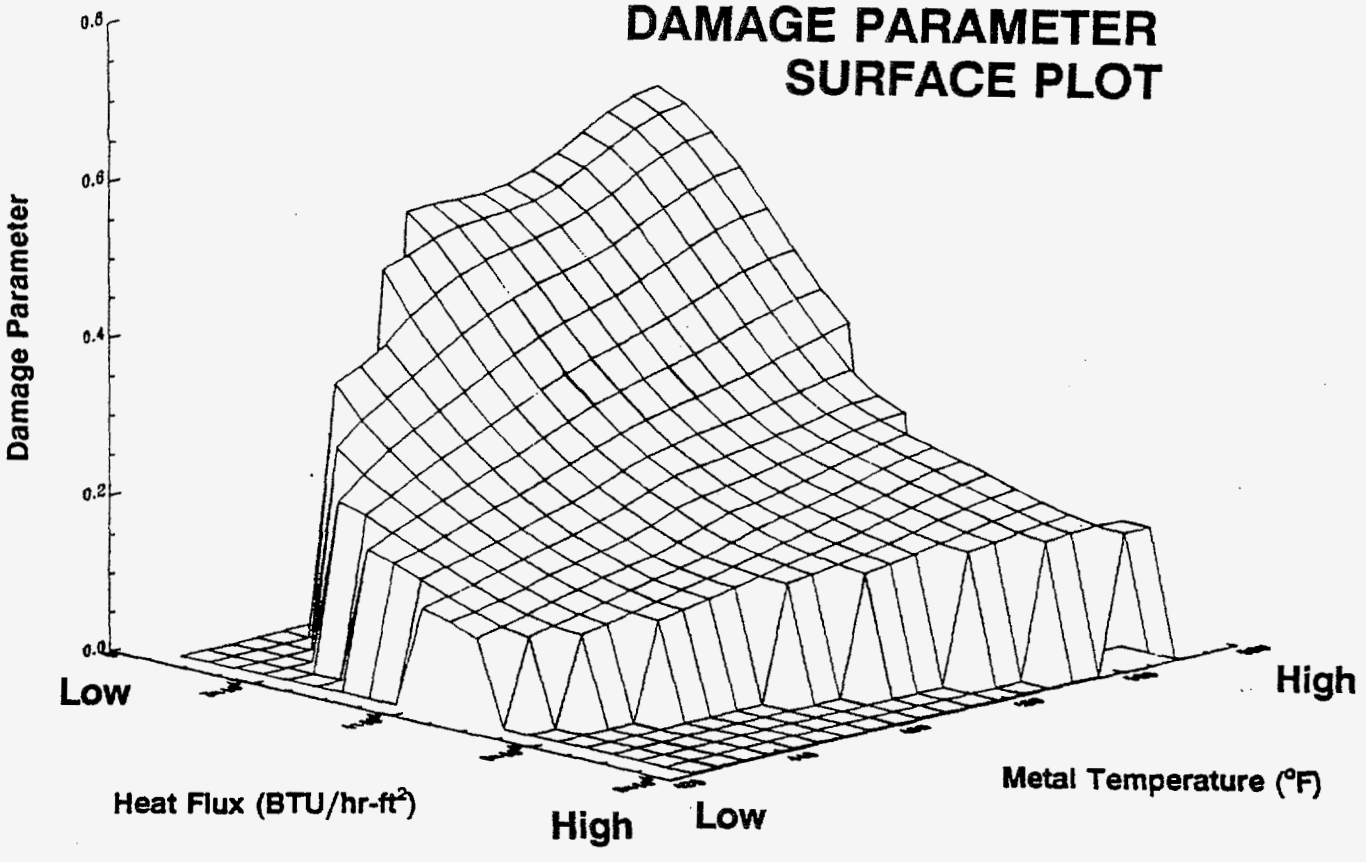

'Damage Parameter' = Concentration Factor (CFACT) x Liquid Collapse Level (CLEV)

Figure 25. Surface Plot of Calculated ECD Damage Parameter.